AD NUMBER

AD817982

LIMITATION CHANGES

TO:

Approved for public release; distribution is unlimited.

FROM:

**Distribution authorized to U.S. Gov't. agencies and their contractors;
Administrative/Operational Use; MAY 1967. Other requests shall be referred to Air Force Inst of Technology, Wright-Patterson AFB, OH 45433.**

AUTHORITY

AFIT ltr 22 Jul 1971

AIR FORCE INSTITUTE OF TECHNOLOGY

AIR UNIVERSITY
UNITED STATES AIR FORCE

PNEUMATIC LINE DYNAMICS

THESIS

GA/ME/67-3

Robert Wencel Wilda
Capt USAF

SCHOOL OF ENGINEERING

WRIGHT-PATTERSON AIR FORCE BASE, OHIO

PNEUMATIC LINE DYNAMICS

THESIS

GA/ME/67-3

Robert Wencel Wilda
Capt USAF

AFLC-WPAFB-JUL 67 35

PNEUMATIC LINE DYNAMICS

Thesis

Presented to the Faculty of the School of Engineering of

the Air Force Institute of Technology

Air University

in Partial Fulfillment of the

Requirements for the Degree of

Master of Science

by

Robert Wencel Wilda, B.S.M.E.

Captain USAF

Graduate Astronautics

May 1967

Preface

This report is a continuation of a thesis written by Lt. James Karem, Jr. (Ref. 6). His work was undertaken as the result of a proposal made to the Air Force Flight Dynamics Laboratory (Ref. 1), and dealt with the amplitude frequency response of blocked, 0.170 in I.D., pneumatic lines.

Since many applications of transmission lines in this category carry some mean air flow, and/or are volume terminated, it was my hope to determine the extent to which the basic theory is applicable under these conditions. All of the theoretical work cited is predicated on no mean air flow in the line, so any results of this report are my own interpretations of experimental observations. Some of the references (Ref. 3, 7, 9 and 10) discuss volume termination, but not in the frequency range covered in this investigation.

I am indebted to my faculty advisor, Dr. Milton Franke, and to my laboratory advisor, Mr. James Hall of the Air Force Flight Dynamics Laboratory. Without their guidance and understanding this report would not have been possible. Also, I wish to thank Mr. Earl Criswell of Zone Shop No. 5 for his help and excellent work in the design and construction of the test fixtures and associated hardware. Finally, I wish to thank my typist, Mrs. Anna L. Lloyd.

Robert W. Wilda

Contents

Contents (Contd)

List of Figures

List of Tables

List of Symbols

A	line cross-sectional area	in^2
C	capacitance/unit length	$\frac{cis\text{-}sec}{psi}/^1in$
c_a	adiabatic sonic velocity	in/sec
d	inside diameter of line	in
d_o	diameter of bleed orifice	in
f	signal frequency	Hz (cycles/sec)
G	conductance per unit length	$\frac{cis}{psi}/in$
I	current	amp
K	attenuation parameter	$\frac{nepers}{\sqrt{Hz}}/in$
L	inductance/unit length	$\frac{psi\text{-}sec}{cis}/in$
$\overline{L}$	total line length	in
N_{Re}	Reynolds number	dimensionless
P	AC pressure (variation about $\overline{P}$)	psi-rms
$\overline{P}$	DC mean pressure	$\frac{lbf}{in^2}$ or psi
$\overline{Q}$	mean volume flow rate	$\frac{in^3}{sec}$ or cis
R	resistance per unit length	$\frac{psi}{cis}/in$
R	gas constant	$\frac{in^2}{sec^2\text{-}R}$
S	signal size	percent
$\overline{T}$	DC temperature	R

[1]Units refer to pneumatic parameters where there is a pneumatic-electric equivalence with respect to symbols.

List of Symbols (Contd)

V	voltage	volt
Vol	terminal volume	in^3
x	coordinate indicating distance from load	in
Y	admittance/unit length	$\frac{cis}{psi}/in$
Z	impedance/unit length	$\frac{psi}{cis}/in$
α	attenuation/unit length	neper/in
β	phase shift/unit length	rad/in
Γ	propagation constant/unit length	1/in
γ	ratio of specific heats	dimensionless
μ	viscosity	psi-sec
ν	kinematic viscosity	$\frac{in^2}{sec}$
λ	wavelength	in
ρ	density	$\frac{lbm}{in^3}$
σ^2	Prandtl number	dimensionless
ω	signal frequency	radians/sec
$( )_{AMB}$	ambient	
$( )_e$	electrical	
$( )_i$	incident	
$( )_{max}$	maximum	
$( )_{min}$	minimum	
$( )_n$	evaluated at $\overline{L} = n\lambda/4$	
$( )_o$	characteristic value	
$( )_r$	evaluated at receiving (load) end	

List of Symbols (Contd)

$( )_{\overline{r}}$	reflected
$( )_s$	evaluated at sending (generator) end
$( )_v$	viscous characteristic
$\simeq$	is approximately equal to
$R_e( )$	real part of
$I_m( )$	imaginary part of

Abstract

The amplitude frequency response was experimentally determined for 0.170 in I.D. flowing pneumatic lines of the type used in flueric systems. Preliminary results are given for 0.073 in I.D. pneumatic lines for both flowing and blocked line conditions. A mean volume flow rate of 2 to 24 cubic inches per second was studied. Line lengths up to 20 feet were studied at mean pressures from 10 to 40 psig. The sinusoidal driving signal frequency was varied from 1 to 1000 Hz, and signal size varied from 0.15 to 15 percent of the mean line pressure.

Test results were compared to the predictions of the high-frequency theory of Karem, which was developed from the work of Nichols and is based on the electric-pneumatic analogy. For signal sizes less than 1 percent, the high-frequency theory predicted resonant gain within 4 db and resonant frequency within 20 percent at all frequencies and for both line sizes. At larger signal sizes, predicted resonant gain was within 6 db and resonant frequency within 20 percent over the frequency range of 100-1000 Hz.

A preliminary check showed the high-frequency theory as applied to blocked lines could not be used to predict the frequency response of a volume terminated line.

PNEUMATIC LINE DYNAMICS

I. Introduction

Background

Over the past several years considerable research and development effort has been given to the design and application of flueric systems, i.e., systems whose operation depends solely on a fluid. Because of their simplicity, light weight, and adaptability to extreme operating conditions, flueric systems are expected to become increasingly important in aerospace applications.

While the frequency response characteristics of individual flueric devices are well known, until the work of Karem (Ref. 6), there had been little experimental work done to verify the theoretically predicted frequency response characteristics of the line used to connect the individual flueric elements. Karem studied the steady state frequency response of short, blocked pneumatic transmission lines (up to 240 in long) at frequencies at 1 to 1000 Hz. His work was preceded by several theoretical studies (Ref. 2, 3, 5, 7, 8, 9, 10, 11, and 12), but these were concerned mainly with very low frequencies (1 to 10 Hz) and lines several hundred feet long. All of the previous work was predicated on the basis of no mean air flow in the transmission line (Ref. 8 and 9). This is often not the case, since many systems employ a vented or flowing line. Also, volume termination studies are not found in literature for the line lengths and frequencies used in Karem's tests.

Electric Analogy

Several of the previous investigators of this problem utilize a pneumatic-electric analogy in their analysis and presentation (Ref. 6, 8, 9, 10, and 14). By using an electric analogy, the methods already developed for electrical transmission lines are made available for the analysis of pneumatic lines. These methods include transmission line charts and analog computer simulation.

Objectives

The objectives of this study were as follows:

1. Determine if the high-frequency theory developed by Karem (Ref. 6) holds for 0.073 in I.D., blocked pneumatic lines. Tests were run on 15 and 30 in lines and the amplitude frequency response was compared to that predicted by Karem's high-frequency theory.

2. Determine the amplitude frequency response of 0.170 in I.D. and 0.073 in I.D. pneumatic lines carrying a mean air flow (i.e., a flowing line). Mean pressures of 10, 25, and 40 psig were used, with sinusoidal (AC) pressure signals of 0.15 to 3 percent of the mean pressure.

3. Determine the effect of volume termination on the frequency response of 0.170 in I.D. pneumatic lines; terminal volumes between 1 and 11 cubic inches were studied.

II. Theory

Electrical Theory

The voltage distribution in an electrical transmission line driven by a sinusoidal generator may be analyzed by the assumption of traveling waves, and is found to be (Ref. 13: 10-15)

$$V = V_i e^{\sqrt{ZY}\ x} + V_{\bar{r}}\, e^{-\sqrt{ZY}\ x} = V_i e^{\Gamma x} + V_{\bar{r}} e^{-\Gamma x} \tag{1}$$

The unit attenuation and unit phase shift may then be defined as

$$\alpha = R_e(\Gamma) \text{ and } \beta = I_m(\Gamma) \tag{2}$$

If the line losses are small, Γ is almost purely imaginary, and α and β can be represented by (Ref. 13:81)

$$\alpha = \frac{LG + RC}{2\sqrt{LC}} \tag{3}$$

$$\beta = \omega\sqrt{LC} \tag{4}$$

When a line is resonant,

$$\beta\bar{L} = n\pi/2 \text{ for } n = 1, 2, 3, \ldots \tag{5}$$

By definition,

$$\omega = 2\pi f \tag{6}$$

Substituting Eq. 4 and 6 into Eq. 5 gives

$$f_n = \frac{n}{4\bar{L}\sqrt{LC}} \tag{7}$$

Further, a transmission line, when driven by a sinusoidal signal, has points of relative maximum and minimum voltage, known as "anti-nodes" and "nodes" respectively, along its length. It may be shown (Ref. 13: 86) that the voltage of the nodal points may be presented by

$$V_{min} = V_r \sinh \alpha x \tag{8}$$

For the anti-nodal voltages,

$$V_{max} = V_r \cosh \alpha x \tag{9}$$

The gain of a line is defined as

$$\text{Gain} = V_r/V_s \tag{10}$$

When V_s is minimum, the gain is maximum, and substitution of Eq. 8 into Eq. 10 with $x = \overline{L}$ results in

$$\text{Gain}_{max} = \frac{1}{\sinh \alpha L} \tag{11}$$

Substitution of Eq. 9 into Eq. 10 results in

$$\text{Gain}_{min} = \frac{1}{\cosh \alpha L} \tag{12}$$

Equations 11 and 12 are the basis of the "gain envelope" technique used in frequency response analysis.

The characteristic impedance of a transmission line is given by (Ref. 13:79)

$$Z_0 = \sqrt{\frac{Z}{Y}} = \sqrt{\frac{R + j\omega L}{G + j\omega C}} \tag{13}$$

When ω is large, this reduces to

$$Z_0 = \sqrt{\frac{L}{C}} \tag{14}$$

When the load impedance, Z_r, is made equal to Z_0, the transmission line will not exhibit resonance, and the voltage maximum and minimum described earlier will not occur. Neglecting resistance, the voltage will remain constant along the line.

High-Frequency Theory

Nichols (Ref. 8), in his pneumatic transmission line model, defined a viscous characteristic frequency as

$$\omega_v = \frac{8\pi\nu}{A} \tag{15}$$

Karem (Ref. 6:10), showed that for high frequencies ($\omega >> \omega_v$), the line elements derived by Nichols (Ref. 8) reduced to

$$R = \frac{1}{2} L \sqrt{\omega\omega_v} \tag{16}$$

$$G = \frac{\gamma-1}{2\sigma} C \sqrt{\omega\omega_v} \tag{17}$$

$$L = \rho/A \tag{18}$$

$$C = A/\gamma\bar{P} \tag{19}$$

$$\alpha = \sqrt{f}\left[\frac{\gamma-1}{\sigma} + 1\right]\sqrt{\frac{\pi 2\mu}{\gamma A\bar{P}}} = \sqrt{f}\ K \tag{20}$$

and

$$\beta = \omega/c_a \tag{21}$$

Rohmann and Grogan (Ref. 9) and Zalmanzon (Ref. 14:251) define a terminal volume capacitance as

$$C_r = \frac{Vol_r}{\bar{P}} \tag{22}$$

$$Z_r = \frac{1}{\omega C_r} = \frac{\bar{P}}{\omega\ Vol} \tag{23}$$

Substituting the pneumatic parameters for R and G, Eq. 16 and 17, into the equation for Z_o, Eq. 13, we find

$$Z_o = \sqrt{\frac{L}{C}} \left[\frac{\omega_v/4 + \omega}{\frac{(\gamma-1)^2}{4\sigma^2}\ \omega_v + \omega} \right]^{\frac{1}{4}} \tag{24}$$

For air, and with $\omega >> \omega_v$, the term in the bracket is nearly equal to one. Therefore

$$Z_o \simeq \sqrt{\frac{L}{C}} \tag{25}$$

Substituting Eq. 18 and 19 for L and C

$$Z_o = \frac{\bar{P}}{A}\sqrt{\frac{\gamma}{RT}} \tag{26}$$

Setting Z_r, Eq. 23, equal to Z_o yields

$$f = \frac{\sqrt{\gamma RT}\ A}{2\pi Vol} = \frac{c_a\ A}{2\pi Vol} \tag{27}$$

This is the frequency for which a given terminal volume will present a load impedance (Z_r) equal to the characteristic impedance (Z_o) of the line.

Signal Size

To be consistent with the work of Karem (Ref. 6), the signal size will be defined to be

$$S = \frac{P\ @\ f = 1\ Hz\ in\ psi\text{-}rms}{\bar{P}\ in\ psig}$$

III. Apparatus

The test system used was essentially the same as used by Karem (Ref. 6), and consisted of a pneumatic signal source, sending and receiving fixtures, the test line, and monitoring equipment. The equipment, except for the fixtures and a switch box, is commerically available and, therefore, will not be described in detail. Major specifications are given in Appendix C. Figure 1 is a schematic of the major components and Figure 2 shows the laboratory set-up.

Pneumatic Signal Source

The pneumatic signal generator used in this experiment was developed by the Bendix Research Laboratories and is now commercially available. The generator is basically an electro-pneumatic valve which uses a piezo-electric disc as the flapper of a variable orifice to produce pneumatic wave modes. The flapper varies the effective metering area between an outlet port and a region of constant supply pressure as the electrical driving signal is varied. The valve is capable of duplicating an input electrical sinusoidal signal pneumatically, with little distortion, at frequencies from 0.1 to over 1000 Hz. Figure 3 is an example of the sinusoidal waveforms obtained from a representative test condition. Signal amplitude can be varied by changing the mean air flow through the pneumatic driver, and by varying the AC input voltage from the low frequency function generator.

Sending and Receiving Fixtures

The sending fixture is shown in Figure 4, and the receiving fixtures are shown in Figures 5 and 6.

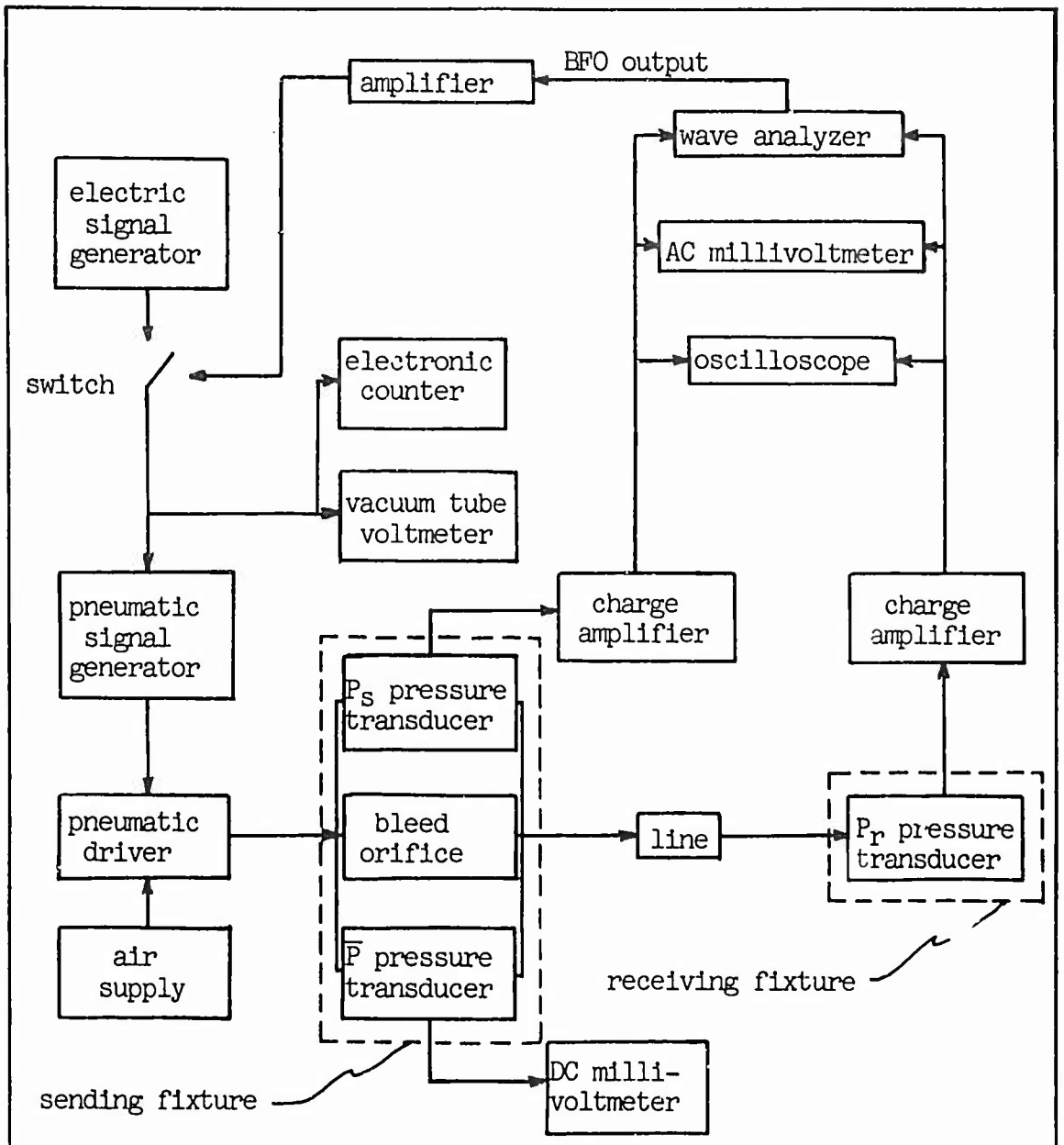

Note: The bleed orifice is located in the receiving fixture for flowing line tests.

Figure 1 Apparatus Schematic

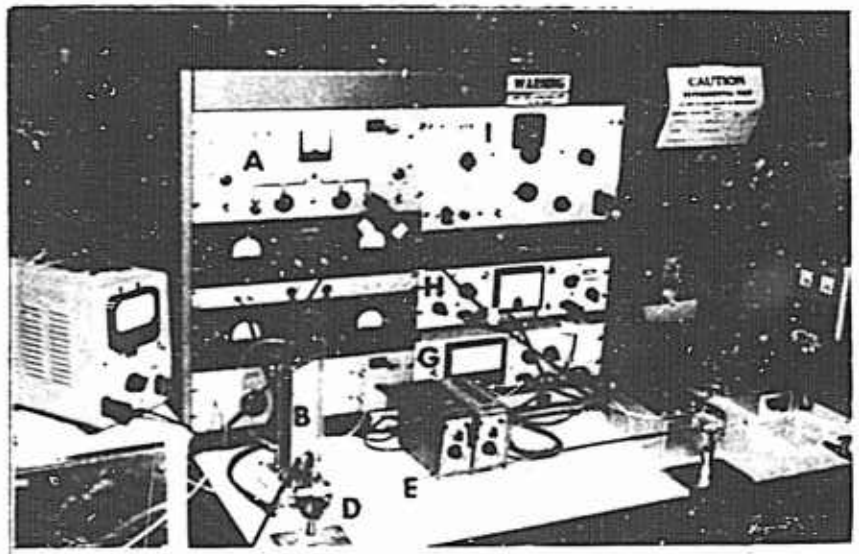

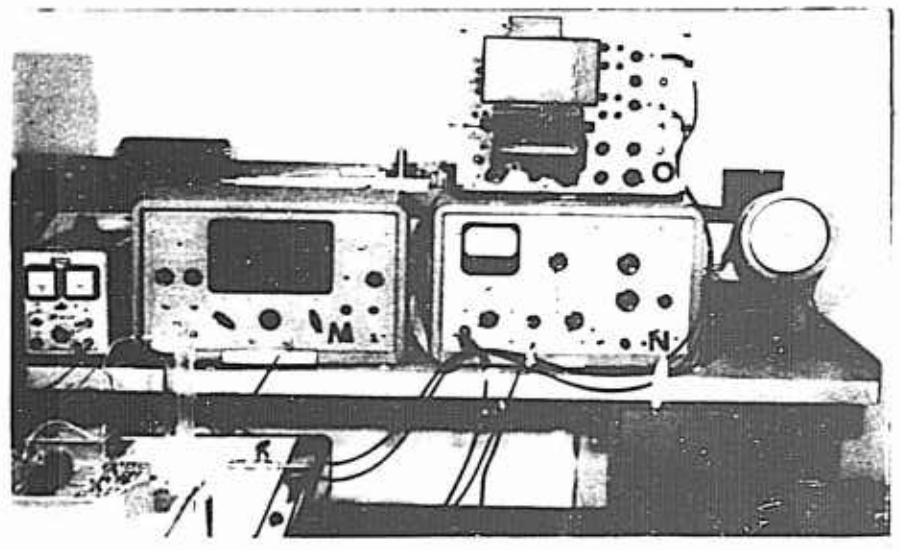

A--pneumatic signal generator
B--flow meter
C--pneumatic driver
D--sending fixture
E--transmission line
F--charge amplifiers
G--DC millivoltmeter
H--AC millivoltmeter
I--electric signal generator
J--receiving fixture
K--amplifier
L--volume receiving fixture
M--electronic counter
N--wave analyzer
O--oscilloscope

Figure 2 General View of Apparatus

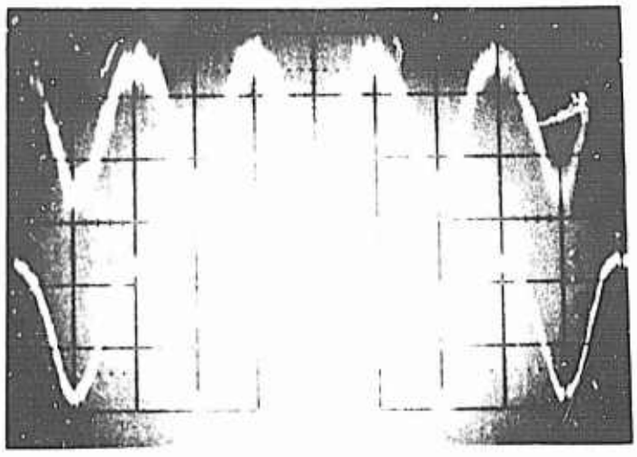

P_s--upper trace P_r--lower trace

$\bar{L}$=15 in, d=0.170 in, $\bar{P}$=40 psig, S=0.2%, f=10 Hz

Figure 3 Typical Scope Trace of Pneumatic Signals

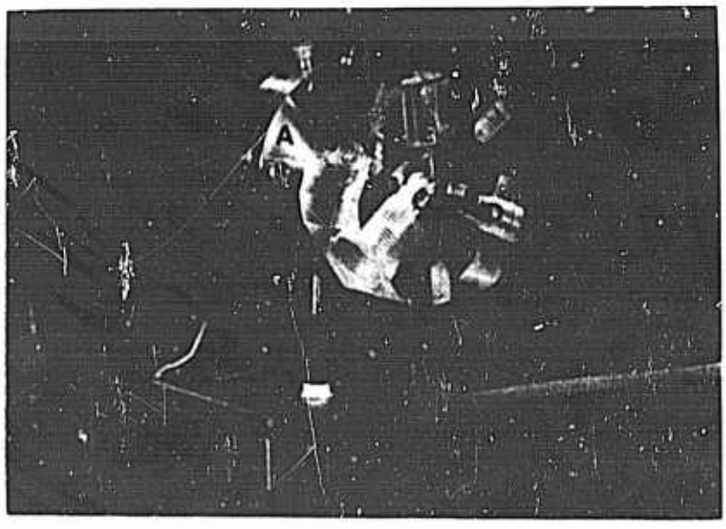

A--pneumatic driver

B--sending fixture

C--$\bar{P}$ pressure transducer

D--P_s pressure transducer

E--bleed orifice

Figure 4 Sending Fixture

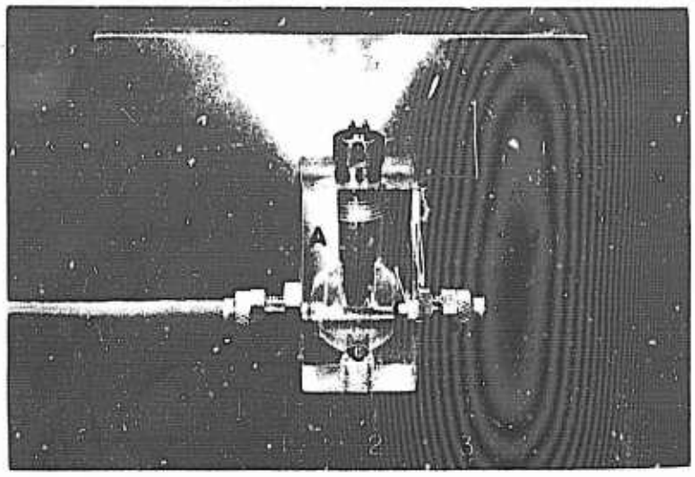

A--blocked and flowing line receiving fixture

B--P_r pressure transducer C--bleed orifice ports

Figure 5 Blocked and Flowing Line Receiving Fixture

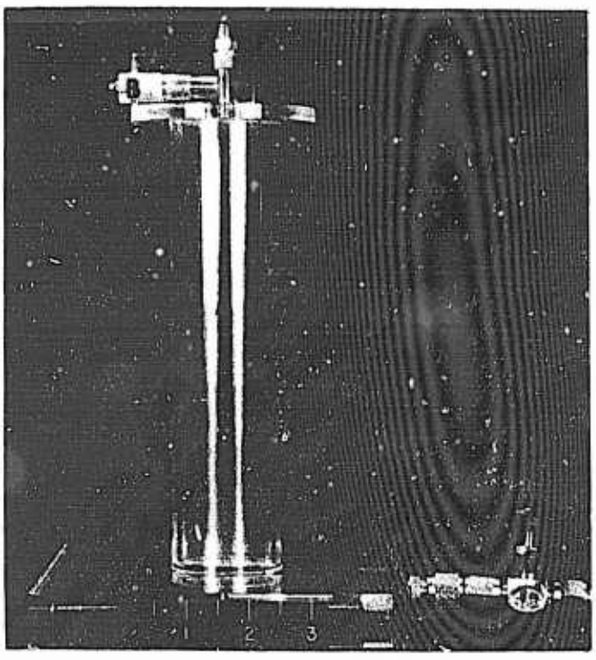

A--volume termination receiving fixture

B--P_r pressure transducer C--water level control

Figure 6 Volume Termination Receiving Fixture

The sending fixture differs from that used in the previous study (Ref. 6) in that the orifice and AC and DC pressure measurement ports are located at the same point on the line, instead of being separated by distances on the order of one inch. The pressure pick up point is also nearer to the driver (ideally it should be at the sending point, but physical design prevented this). The orifice port in the sending fixture is designed to accept different size orifices; the port can also be blocked for use of the fixture in the flowing line tests.

Two receiving fixtures were used; one for the blocked and flowing line tests and the other for volume termination tests. The flowing line fixture was designed so an orifice could be placed perpendicular to, or parallel to, the axis of the line. For blocked line tests, both orifice ports were closed. In the volume termination fixture, a variable water level was used to adjust the terminal volume.

The fixtures were designed so that their internal diameter matched that of the line throughout. The pressure transducers were mounted 0.020 in above the bottom of a cavity, and a 1/8 in long by 1/16 in diameter tap connected the cavity to the line. Various sized orifices were used to produce signal sizes of 0.15 to 20 percent.

Line

Imperial Eastman "Poly-Flo" plastic tubing was used for all tests. Lengths of 15, 30, 60, 90, 120, 180, or 240 inches were used; however, not all lengths were tested at all of the possible operating conditions. Line length was measured between the P_r and P_s pressure taps. The longer lines were smoothly coiled around a two-foot-diameter drum for convenience. Both 1/4 in O.D., 0.170 in I.D. and 1/8 in O.D.,

0.073 in I.D. lines were used in the flowing and blocked line tests. In the volume termination tests, only the 0.170 in I.D. lines were used.

Monitoring Equipment

Electrical signal input frequency was monitored by an electronic counter. The output of the DC pressure transducer ($\overline{P}$) was monitored by a differential millivoltmeter. The output of the AC pressure transducers (P_r and P_s) is a varying charge which is amplified and converted to a varying voltage by charge amplifiers. This signal was then measured in one of three possible ways. An oscilloscope was used for visual observation of both AC signals at all times, and pictures of the traces were made for amplitude measurements of the signals when required. A phase angle voltmeter was used as an AC millivoltmeter to determine the total signal amplitude at frequencies above 10 Hz. A wave analyzer was used to determine the amplitude of the fundamental component of the signals at frequencies above 20 Hz. A converted altimeter was used to measure ambient pressure ($\overline{P}_{AMB}$) and a mercury-in-glass thermometer was used to measure ambient temperature ($\overline{T}_{AMB}$).

Miscellaneous

Air used in these tests was obtained from the laboratory air supply. Two in-line filters and a settling tank were used to ensure a clean, steady air supply. The filtered air could only be described as "not excessively moist", since no method was available to thoroughly dry the air.

IV. Procedure

Since the sending signal (P_s) pressure transducer could not be placed at the sending end reflection point, the condition for a maximum sending signal did not coincide with that for minimum gain. This was especially true for the shorter lines, where a frequency difference on the order of 20 Hz was observed between maximum P_s and minimum gain.

Due to harmonics which occur near the line resonance points, only the wave analyzer could be used to measure the fundamental response near these points. The wave analyzer would not function accurately at frequencies below 20 Hz, so no readings were taken below this frequency when a line was near resonance.

The electrical input signal was obtained from the low frequency function generator at frequencies below 20 Hz, and from the Beat Frequency Oscillator (BFO) in the wave analyzer at frequencies above 20 Hz. Use of the BFO simplified the testing considerably, since the wave analyzer was then continuously reading at the same frequency as the input electrical signal. This procedure enabled the resonance points to be quickly found, since P_s could be monitored continuously as a function of frequency, and the maximum and minimum values could be readily observed.

Tests were run using bleed orifices of 0.013, 0.20, and 0.052 in diameter. The 0.052 in diameter orifice was the largest that could be used in the tests while still maintaining a DC line pressure ($\overline{P}$) of 10 psig; this limitation was imposed by the available air supply. Blocked line tests were run in order to correlate with the results of

Karem (Ref. 6). Tests were run on line lengths of 15, 30, 90, 180 and 240 in; the 0.013 and 0.020 in diameter orifices were used for the small signal tests, and the 0.052 in diameter orifice was used for the large signal tests. As the signal frequency was varied from 1 to 1000 Hz, the signal amplitude was measured at the sending and receiving end of the line. Measurements were taken at intervals up to the first minimum gain point, and at gain maxima or minima from that point out to 1000 Hz.

V. Results and Discussion

A sample calculation for determination of the gain envelope using the high-frequency theory is given in Appendix A. Flow rate calculations are also shown. Gain curves and data for all experimental tests are given in Appendix B.

Blocked Line

Initially, tests were run with 0.170 in O.D. blocked lines to determine the effects of the new sending and receiving fixtures used in this study. These results were compared to Karem's (Ref. 6). Figure 7 gives a comparison of the gain and resonant frequencies of a typical line. The figure shows that gain at resonance is practically unchanged for the two sets of fixtures. However, the resonant frequencies are lower for the new fixtures, and the difference increases with increasing frequency. Since the upper resonant frequencies are (ideally) even multiples of the first resonant frequency, it is seen that a difference of one Hz at the first resonant frequency could, for example, become a difference of 20 Hz at a frequency 20 times the first resonant frequency. For all comparison tests made, resonant frequency was found to follow the same trend as shown in Figure 7. In all cases, however, the resonant frequencies were within 10 percent of that predicted by the high-frequency theory, and gain within 2 db of that predicted by the theory.

Blocked line tests were run on the 0.073 in I.D. line for lengths of 15 and 30 in. Figure 8 gives a typical experimental gain curve, along with the high-frequency theory gain envelope. The experimental

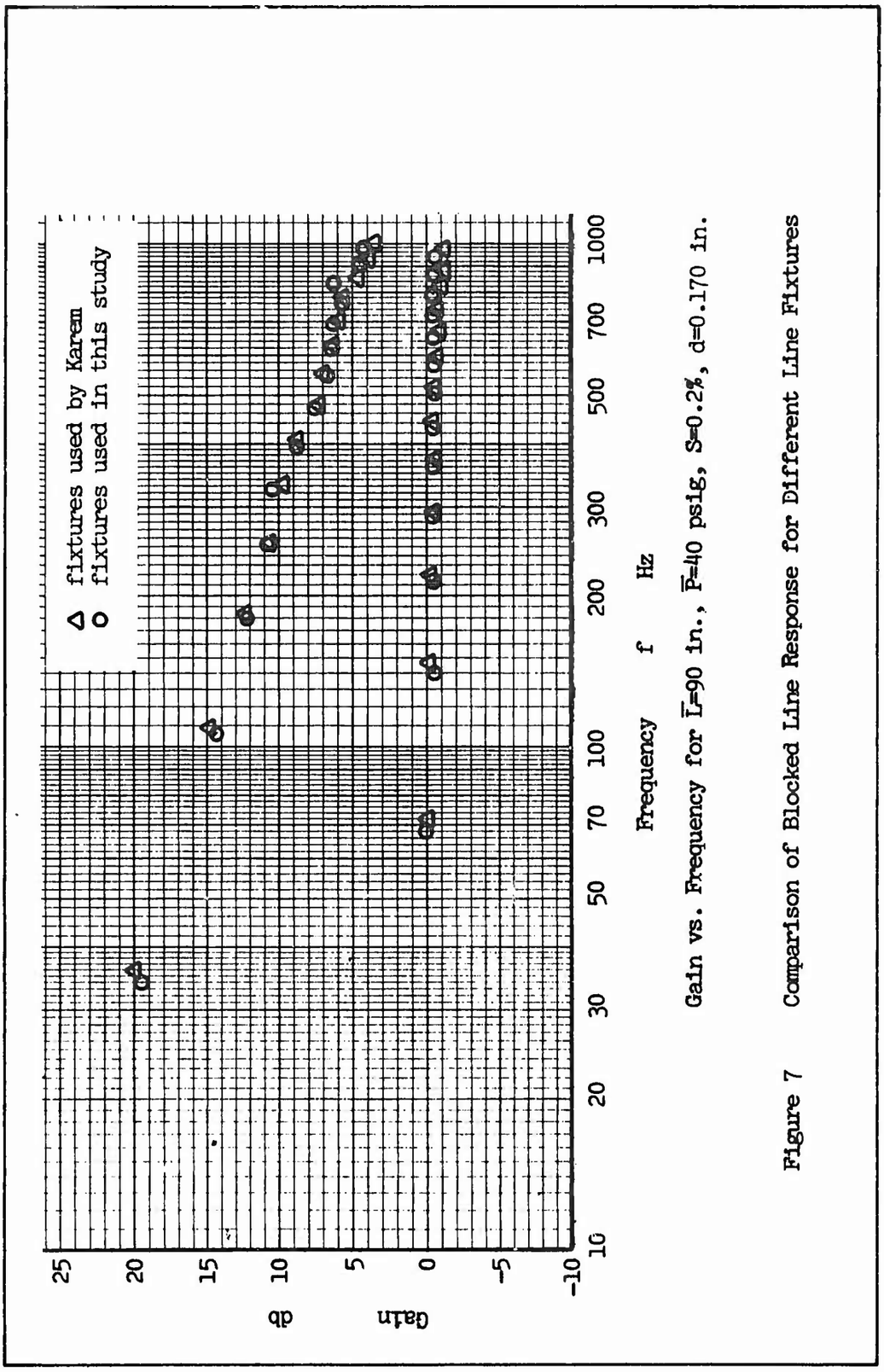

Gain vs. Frequency for $\bar{L}$=90 in., $\bar{P}$=40 psig, S=0.2%, d=0.170 in.

Figure 7 Comparison of Blocked Line Response for Different Line Fixtures

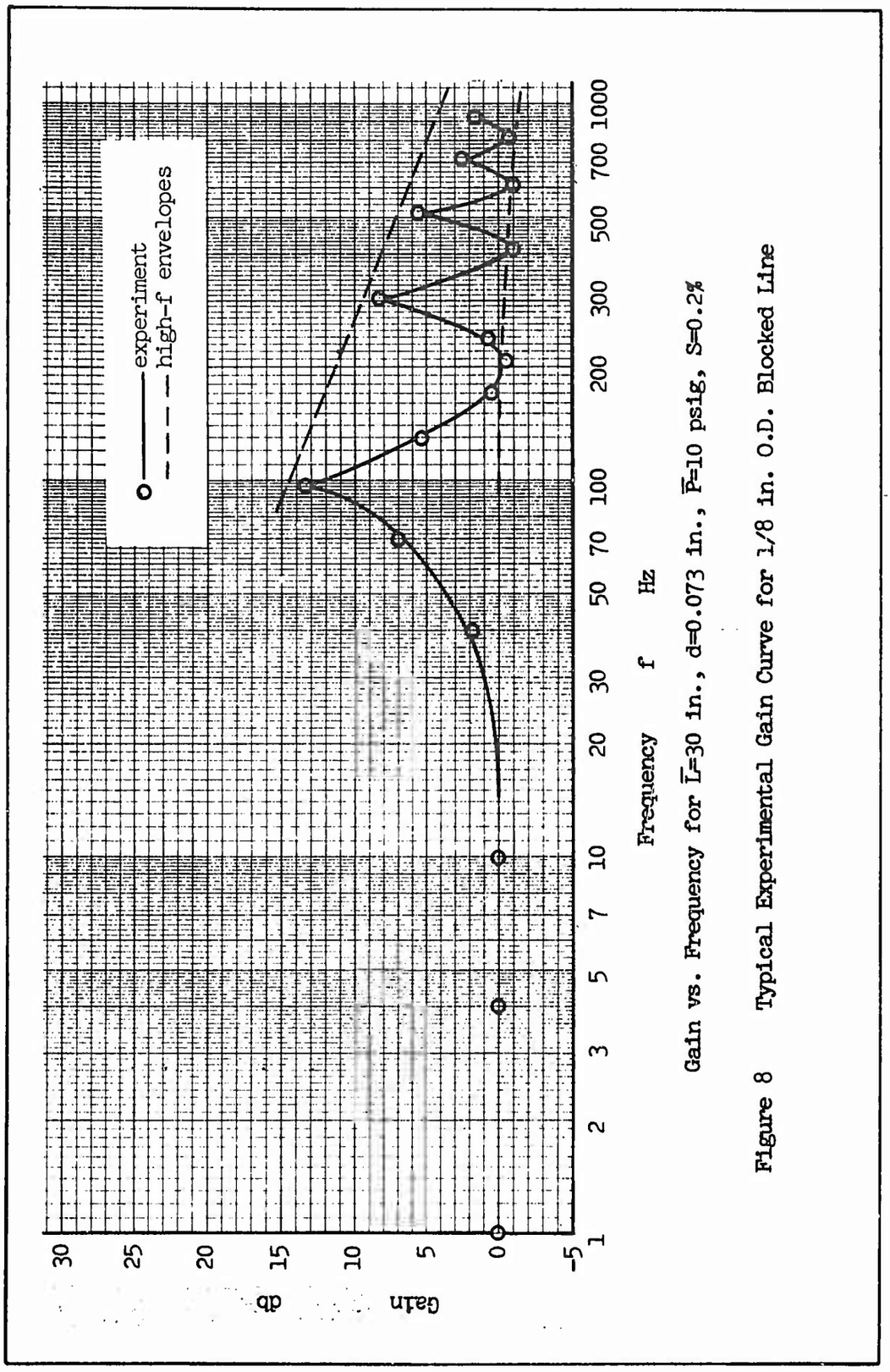

Gain vs. Frequency for $\bar{L}$=30 in., d=0.073 in., $\bar{P}$=10 psig, S=0.2%

Figure 8 Typical Experimental Gain Curve for 1/8 in. O.D. Blocked Line

results indicate that the difference between high-frequency theory and experiment is slightly greater for the 0.073 in I.D. lines than for the 0.170 in I.D. lines. Maximum deviation observed shows the gain to be no more than 4 db below that predicted by the high-frequency theory and resonant frequency to be a maximum of 20 percent below that predicted by the theory.

Flowing Line

Figure 9 compares the frequency response of a typical line for various operating conditions. The figure shows that flow has relatively little effect on frequency response except for the combination of large signal size with a high flow rate. In this instance, maximum gain was appreciably below that predicted by the high-frequency theory at frequencies below 100 Hz. This effect became more pronounced as line length increased. Other than the condition just mentioned, the flowing line tests indicated a maximum decrease in gain of 2 db over the blocked line tests, and essentially no change in resonant frequency. It was also found that the frequency response was the same for the flow orifice placed perpendicular to or parallel to the longitudinal axis of the test line.

Volume Termination

Figure 10 gives an example of the test results for a given line length with different terminal volumes. The high-frequency envelopes are shown on the figure to give an indication of the effects of volume termination. Since the high-frequency theory was derived on the basis of blocked lines, it was expected the results would not fall within the envelopes.

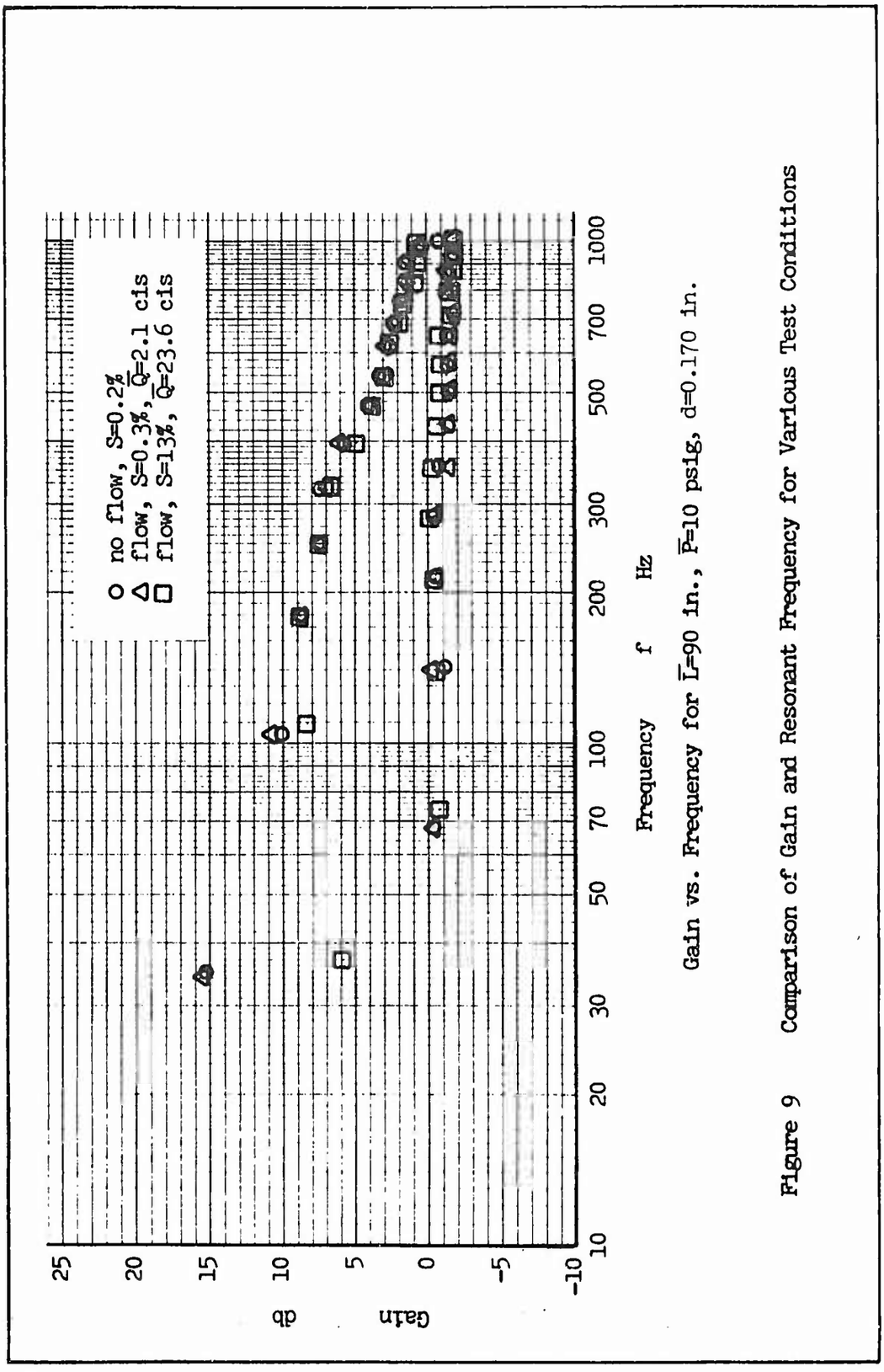

Gain vs. Frequency for $\bar{L}$=90 in., $\bar{P}$=10 psig, d=0.170 in.

Figure 9 Comparison of Gain and Resonant Frequency for Various Test Conditions

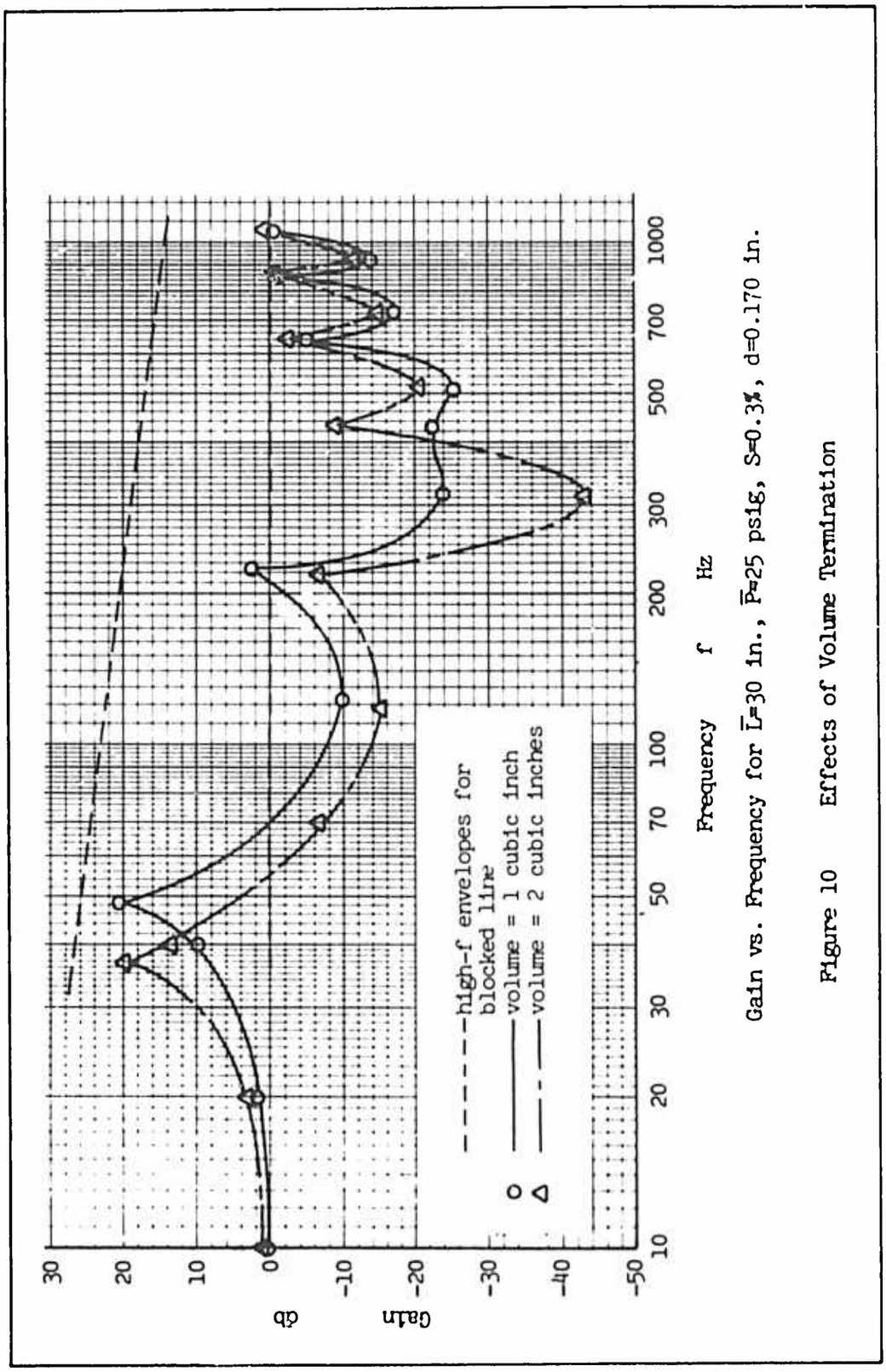

Figure 10 Effects of Volume Termination

Gain vs. Frequency for $\bar{L}$=30 in., $\bar{P}$=25 psig, S=0.3%, d=0.170 in.

Analysis of Results

A summary of results for blocked and flowing lines is presented in Table I. It should be noted that these are maximum deviations, and many deviations were smaller than those given in the table. The deviation would also be smaller than that shown if Nichols' theory (Ref. 8) were used as a basis for comparison since, as stated by Karem (Ref. 6: 32), the high-frequency theory may give gain up to 2 db high and resonant frequency up to 10 percent high over the values predicted by Nichols' theory.

No convenient explanation has been found for the large deviation observed in the tests involving a large signal combined with a high flow rate. One interesting observation is that the experimental response begins to agree with the high-frequency theory at a frequency such that the wave length ($\lambda = c_a/f$) is less than the line length.

A more detailed mathematical analysis is necessary in order to interpret the volume termination results. Another source of difficulty may lie in the fixture design. Since the load impedance (Z_r) is continuously changing with frequency, the value of Z_r goes from above the characteristic impedance (Z_o) to very much less than Z_o as the frequency increases. From electric transmission line theory (Ref. 13:83, 91) this condition causes a continuous change in the phase angle between voltage, current, and impedance, and a consequent change in phase of the standing waves on the line.

Table I

Maximum Deviation Between High-Frequency Theory and Experimental Results for Various Test Conditions

Line I.D.	Test Condition	Gain Deviation (Theory) Minus Experiment)	Resonant Frequency Deviation (% Experimental Value)
0.073 in	blocked	+ 4 db	120%
0.073 in	flowing (small signal; S<1%)	+ 6 db	120%
0.170 in	blocked	+ 2 db	110%
0.170 in	flowing (small signal)	+ 4 db	110%
0.170 in	flowing (large signal; S<1%)	+ 4 db * (f>100 Hz)	110%

* Below 100 Hz, it is a function of line length; + 4 db for $\bar{L}$ = 30 in up to + 15 db at $\bar{L}$ = 180 in

VI. Conclusions

1. The high-frequency theory predicted resonant gain amplitude within 4 db and resonant frequency within 20 percent of experimental values for 0.073 in I.D. 15- and 30-in blocked lines.

2. The high-frequency theory is applicable to flowing lines with zero terminal volume. Except for the case of large signal size at frequencies below 100 Hz, resonant gain amplitude was predicted within 6 db and resonant frequency within 20 percent for both 0.170 in I.D. and 0.073 in I.D. lines. This conclusion holds for flow rates up to at least 24 cubic inches per second and signal size up to at least 15 percent. Correlation was generally better than stated above for small signal size ($S<1\%$), and also better for 0.170 in I.D. lines than for 0.073 in I.D. lines.

3. Accuracy of predicted resonant gain amplitude and resonant frequency can be increased by a factor of about 1/3 when Nichols' theory is used rather than the high-frequency theory.

4. Volume termination has a significant effect on the frequency response of blocked pneumatic lines. Additional theoretical analysis and testing is necessary to arrive at a means of predicting the frequency response of a volume terminated line at the frequencies used in this study.

VII. Recommendations

Application

This study demonstrates that for engineering purposes, the high-frequency theory and associated gain envelope technique for predicting the amplitude frequency response of blocked pneumatic lines of the type used in flueric systems, is applicable to 0.073 in I.D. lines as well as the 0.170 In I.D. lines. Also, the theory can be used when either line is terminated with negligible volume but with a small vent or orifice placed perpendicular to or parallel to the longitudinal axis of the test line.

The study suggests that one means of controlling the maximum gain of a line is to select a line of proper diameter, since for a given line length and mean pressure, the maximum gain is less for a smaller diameter line.

Further Investigations

The comments of Karem (Ref. 6:33) are still valid in this area. The following, somewhat more specific, list of topics is suggested:

(1) The theoretical aspects of load termination should be thoroughly determined, both with characteristic impedance loading and at other load impedance values. A given terminal volume represents the characteristic impedance at only one frequency.

(2) The effects of terminal volume geometry, such as length to area ratio, should be investigated. Pressure transducer location affects should also be evaluated.

(3) A study of signal pressure along the line is possible with the fixtures presently available.

(4) The flowing line results should be verified for high mean pressure with large signal size. This would require a greater air capacity than i available at the present test facility.

Bibliography

1. The Bendix Corporation, Research Laboratories Division. "Investigation of Signal Transmission through Pneumatic Lines". Proposal No. 2283 (1964).

2. Bradner, M. "Pneumatic Transmission Lag". Instruments, 22: 618-625 (1949).

3. Esterson, G. L. "Fluid-Filled Conduit Frequency Response". Proceedings of the 1963 Joint Automatic Control Conference: 328-339.

4. Hilsenrath, J., et al. Tables of Thermal Properties of Gases, Washington, D. C.: National Bureau of Standards Circular 564, 1955.

5. Iberall, A. S. "Attenuation of Oscillatory Pressures in Instrument Lines". Journal of Research, National Bureau of Standards, 45: 85-108 (1950).

6. Karem, J. T., Jr., "The Frequency Response of Blocked Pneumatic Lines", Wright-Patterson AFB, Ohio: Air Force Institute of Technology, M.S. Thesis, GAM/ME/66B-3, 1966.

7. Moise, J. C. "Pneumatic Transmission Lines". Instrument Society of America Journal, 1:35-40 (1954).

8. Nichols, N. B. "The Linear Properties of Pneumatic Transmission Lines". Transactions of the Instrument Society of America, 1:5-14 (1962).

9. Rohmann, C. P., and E. C. Grogan. "On the Dynamics of Pneumatic Transmission Lines". Transactions of the American Society of Mechanical Engineers, No. 2, 79:853-874 (1957).

10. Samson, J. E. "Dynamic Characteristics of Pneumatic Transmission". Transactions of the Society of Instrument Technology, 10: 117-134 (1958).

11. Schuder, C. B., and R. C. Binder. "The Response of Pneumatic Lines to Step Inputs". Transactions of the American Society of Mechanical Engineers, Series D, 81:578-584 (1959).

12. Schuder, C. B., and G. C. Blunk. "The Driving Point Impedance of Fluid Process Lines". Transactions of the Instrument Society of America, 2:39-45 (1963).

13. Skilling, H. H. Electric Transmission Lines, New York: McGraw-Hill Book Company, Inc., 1951.

Bibliography (Contd)

14. Zalmanzon, L. A. Components for Pneumatic Control Instruments, Oxford, Pergamon Press Ltd., 1965.

Appendix A

Sample Calculations

Preliminary Calculations

For a representative condition, use the flowing line test with

$$d = 0.170 \text{ in.}, \ \bar{L} = 30 \text{ in.}, \ \bar{P} = 10 \text{ psig}, \ d_o = 0.013 \text{ in.}$$

Ambient conditions were

$$\bar{T}_{AMB} = 80^{o}F \text{ and } \bar{P}_{AMB} = 14.2 \text{ psia}$$

then $\bar{T} = 80 + 460 = 540^{o}R$

and $\bar{P} = 10 + 14.2 = 24.2$ psia

Using the ideal gas law,

$$\rho = \frac{\bar{P}}{R\bar{T}} = \frac{24.2}{(53.3)(144)(32.3)\ 540} = 1.82 \cdot 10^{-7} \ \frac{lbf\text{-}sec^2}{in^4}$$

With these conditions, air has the properties

$$\mu = \frac{(1.076)(1.153 \cdot 10^{-5})}{(32.2)(144)} = 2.67 \cdot 10^{-9} \text{ psi-sec} \qquad \text{(Ref. 4:26,69)}$$

$$c_a = (1.048)(12)(1087.4) = 1.368 \cdot 10^{4} \text{ in/sec} \qquad \text{(Ref. 4:26,65)}$$

$$\gamma = 1.402 \qquad \text{(Ref. 4:59)}$$

$$\sigma^2 = 0.708, \ \sigma = 0.841 \qquad \text{(Ref. 5:71)}$$

Other parameters are

$$A = \frac{\pi}{4} d^2 = \frac{\pi}{4} (0.170)^2 = 2.27 \cdot 10^{-2} \text{ in}^2$$

$$\nu = \frac{\mu}{\rho} = \frac{2.67 \cdot 10^{-9}}{1.82 \cdot 10^{-7}} = 1.47 \cdot 10^{-2} \text{ in}^2/\text{sec}$$

High Frequency Solution

The attenuation parameter is

$$K = \left[\frac{\gamma - 1}{\sigma} + 1\right]\sqrt{\frac{\pi^2 \mu}{\gamma A \bar{P}}} = \left[\frac{1.4020 - 1}{0.841} + 1\right]\sqrt{\frac{\pi^2 (2.67 \cdot 10^{-9})}{(1.402)(2.27 \cdot 10^{-2})(24.2)}}$$

$$K = 2.74 \cdot 10^{-4} \frac{\text{nepers}}{H_z} \text{/in}$$

For f = 900 Hz, the unit attenuation is

$$\alpha = \sqrt{f}\ K = \sqrt{900}\ (2.74 \cdot 10^{-4}) = 8.22 \cdot 10^{-3} \text{ nepers/in}$$

The total attenuation is

$$\alpha \bar{L} = (8.22 \cdot 10^{-3})(30) = 0.2466 \text{ nepers}$$

The maximum gain is

$$\text{Gain}_{max} = \frac{1}{\sinh\ \alpha \bar{L}} = \frac{1}{\sinh\ 0.2466} = \frac{1}{0.249} = 4.0 = 12.0\text{db}$$

The minimum gain is

$$\text{Gain}_{min} = \frac{1}{\cosh\ \alpha \bar{L}} = \frac{1}{\cosh\ 0.2466} = \frac{1}{1.0306} = 0.97 = -0.3\text{db}$$

The resonant frequencies are

$$f = \frac{nc_a}{4\bar{L}} = \frac{n(1.368 \cdot 10^4)}{4(30)} = 114.0n \text{ Hz for } n = 1, 2, 3, \ldots$$

The calculation for maximum and minimum gain is then repeated for as many frequencies as are necessary to cover the range of interest.

The gain in db verses the corresponding frequency is then plotted on semi-log paper; the maximum gain points are connected together, and the minimum gain points are connected together, thereby forming the gain envelope.

Flow Rate Calculations

For the R-2-15-B "sho-rate" flowmeter, with the stainless steel float, the test readings were

$$p = 12 \text{ psig, flow} = 4.3 \text{ cm}$$

From the manufacturer's data

Temp correction = 0.99, pressure correction = 1.32, and standard flow = 1,700 cc/min

Then

$$\overline{Q} = \frac{(1700)(0.99)(1.32)(0.061 \text{ in}^3/\text{cc})}{60} = 2.26 \text{ in}^3/\text{sec}$$

The flow Reynolds number is

$$N_{Re} = \frac{\overline{Q}d}{A\nu} = \frac{(2.26)(0.170)}{(2.27 \cdot 10^{-2})(1.47 \cdot 10^{-2})} = 1150$$

Signal Size

$$S = \frac{P \text{ @ } f = 1\text{Hz}}{\overline{P}} = \frac{0.026}{10} = 0.0026 = 0.26\%$$

Appendix B

Complete Experimental Data and Gain Curves

Following are the experimental data and gain curves for all tests conducted. Included on the gain curves are the gain envelopes predicted by Karem's high-frequency theory. The following points are pertinent:

(1) The output of the pneumatic generator is not exactly flat and is a function of electrical signal input size.

(2) Tests were run at a constant electrical signal input to the pneumatic generator. This caused a slight variation in pneumatic signal size. The variation was no more than 0.1 percent for the series of runs for any given line.

(3) Most data points were taken at maximum or minimum gain frequencies. The data do not necessarily reflect maximum or minimum pressure at either the sending or receiving AC pressure transducers.

(4) Flowing line results are indicated by the presence of a value for volume flow rate ($\overline{Q}$). Since the frequency response was not affected by the orientation of the flow orifice, all data shown with the exception of Figure B-12 was taken with the orifice perpendicular to the longitudinal axis of the line.

Test ambient temperature ranged from 73 F to 80 F, with a maximum variation of 3 F for any given test. Ambient pressure ranged from 28.73 to 29.91 inches of mercury absolute. The ambient pressure variation was no greater than 0.2 inches of mercury for any given test.

For frequencies between 1 and 10 Hz, data was taken from oscilloscope traces; between 10 and 20 Hz, data was taken with the AC millivoltmeter; and for frequencies greater than 20 Hz, data was taken with the wave analyzer. AC voltage, corresponding to AC pressure, was read to the nearest half of the smallest scale division. Frequency was read to the nearest Hz, since that was as close as a maxima or minima could be located with the frequency adjustment of the wave analyzer.

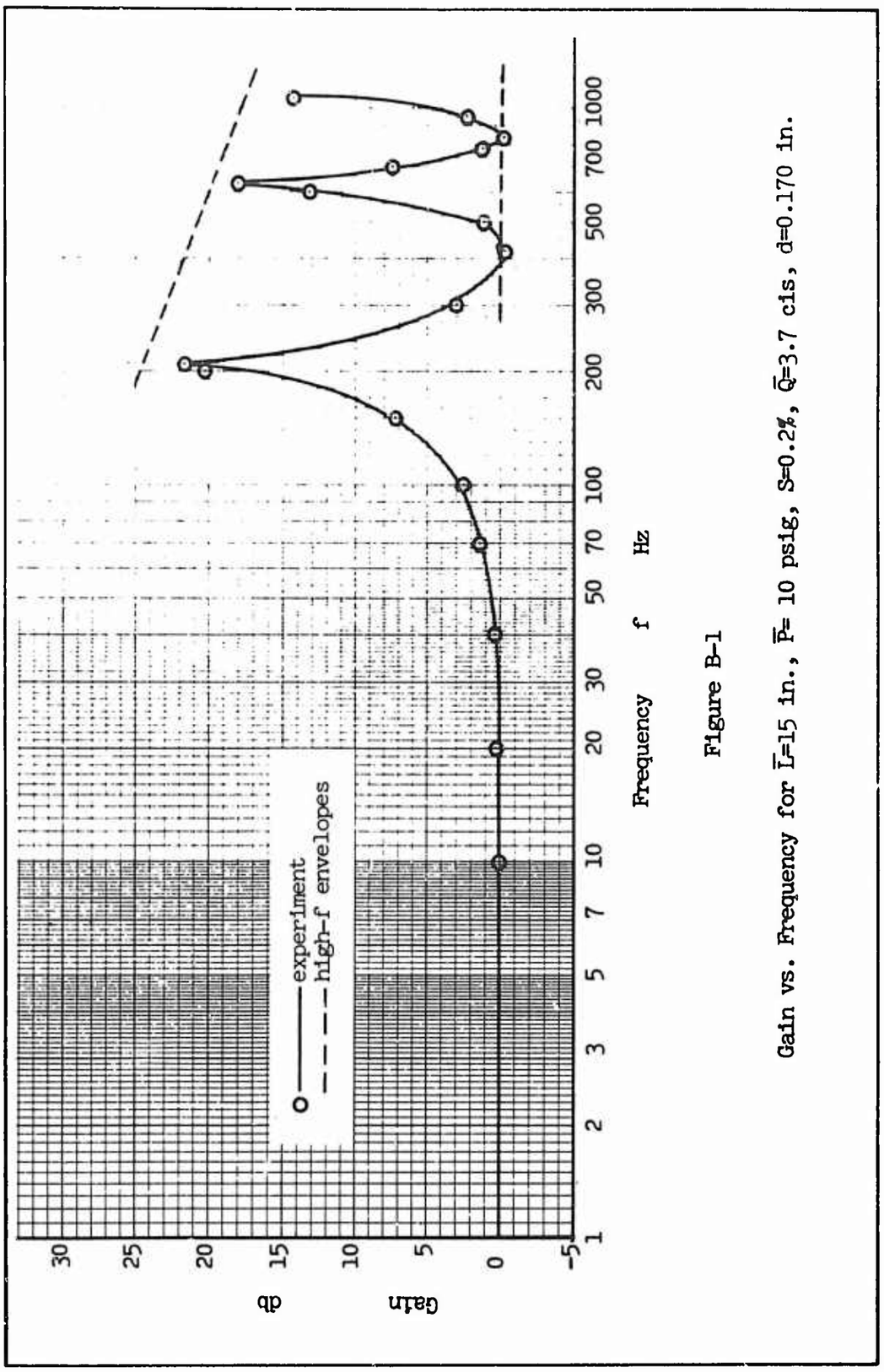

Figure B-1

Gain vs. Frequency for $\bar{L}$=15 in., $\bar{P}$= 10 psig, S=0.2%, $\bar{Q}$=3.7 cis, d=0.170 in.

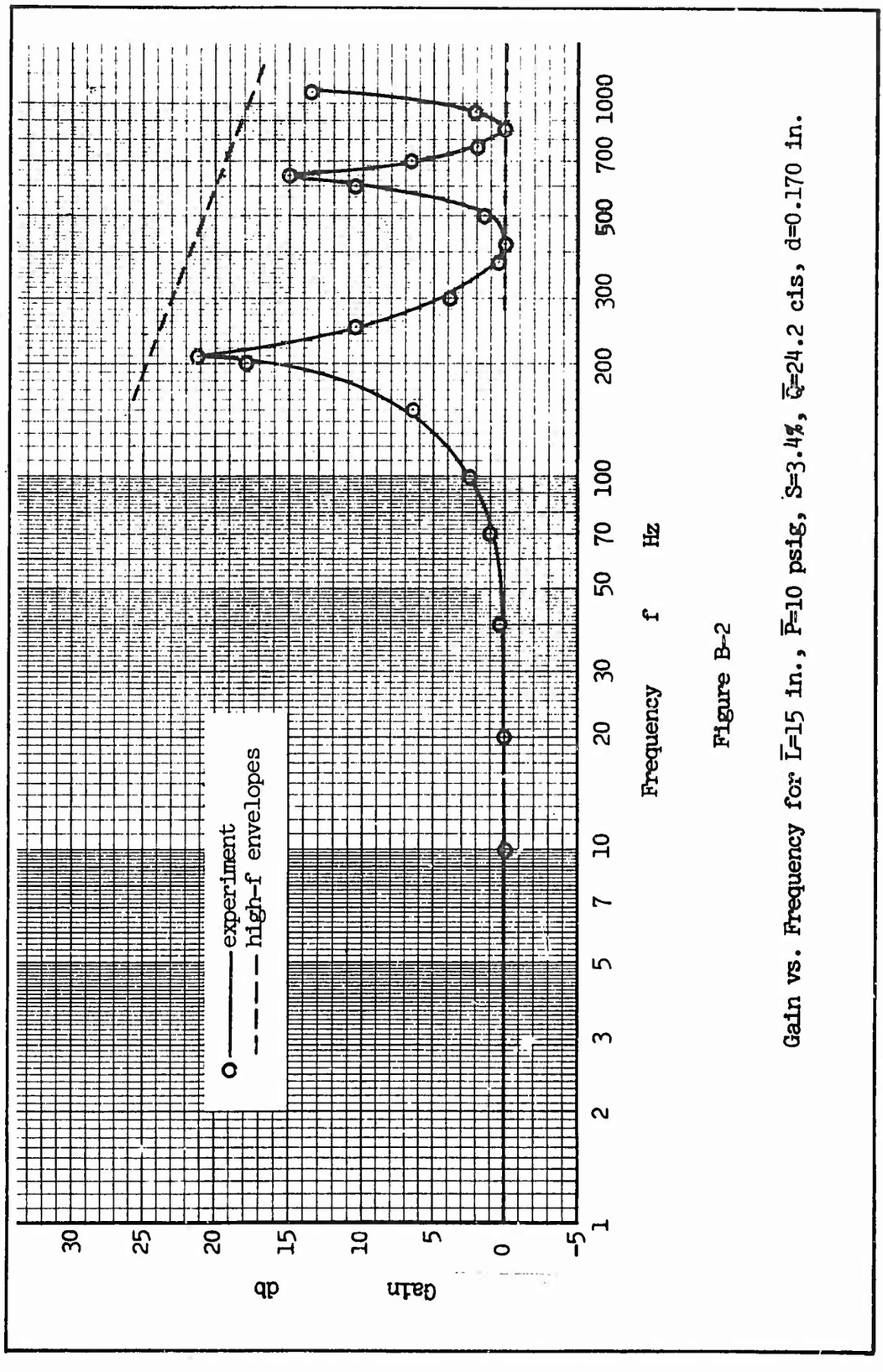

Figure B-2

Gain vs. Frequency for $\bar{L}$=15 in., $\bar{P}$=10 psig, $\bar{s}$=3.4%, $\bar{Q}$=24.2 cis, d=0.170 in.

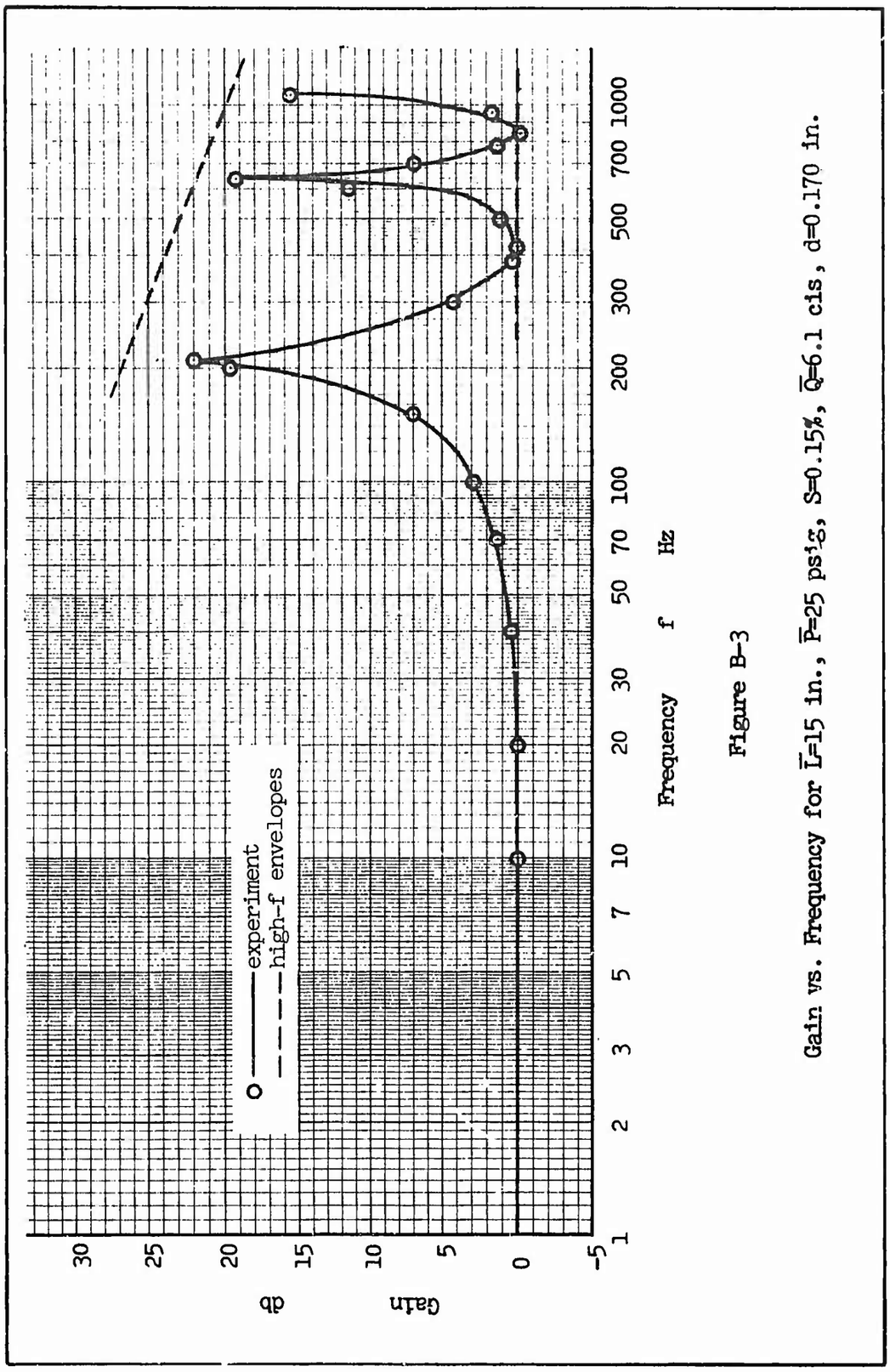

Figure B-3

Gain vs. Frequency for $\bar{L}$=15 in., $\bar{P}$=25 psig, S=0.15%, $\bar{Q}$=6.1 cis, d=0.170 in.

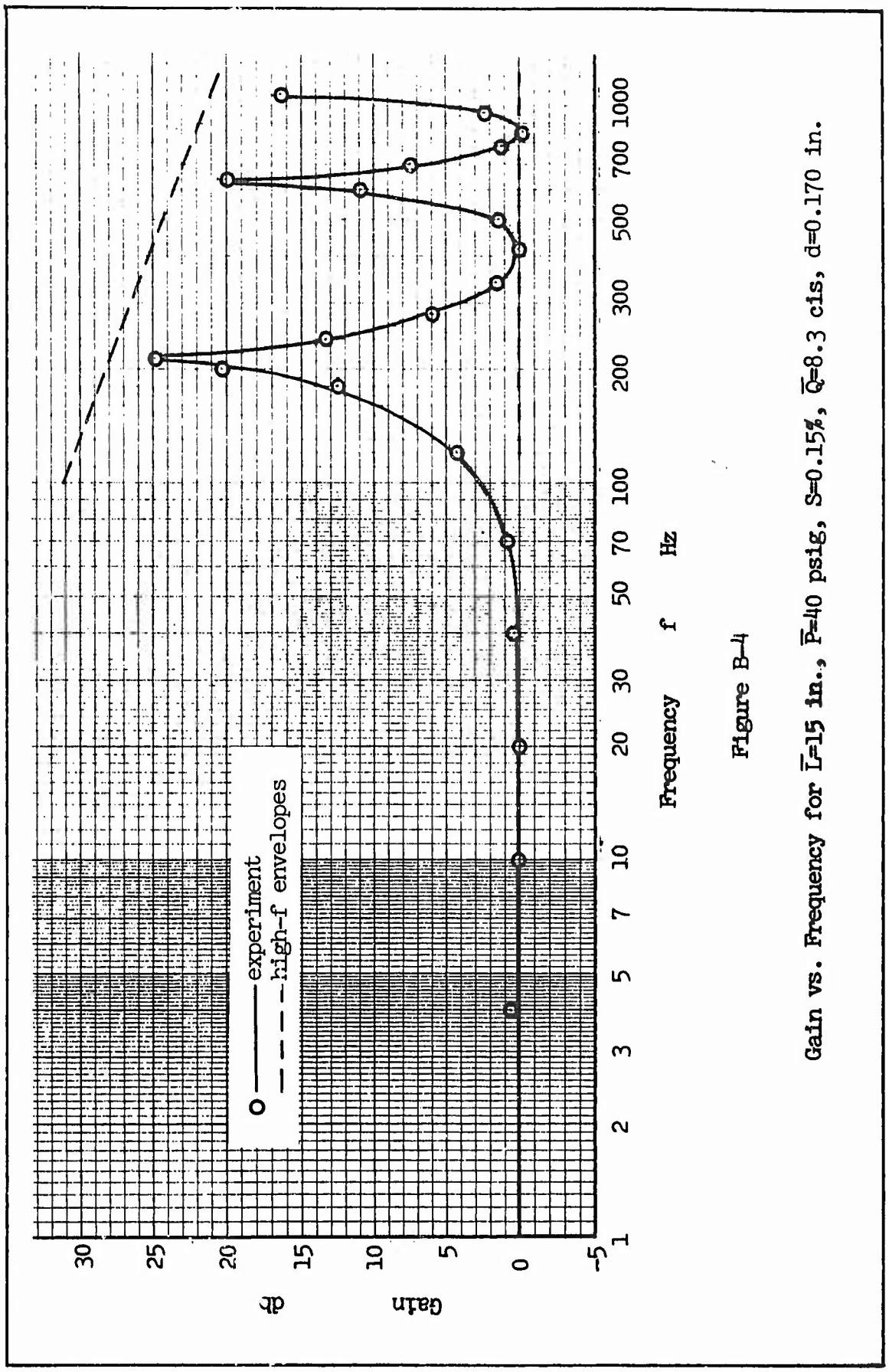

Figure B-4

Gain vs. Frequency for $\bar{L}$=15 in., $\bar{P}$=40 psig, S=0.15%, $\bar{Q}$=8.3 cis, d=0.170 in.

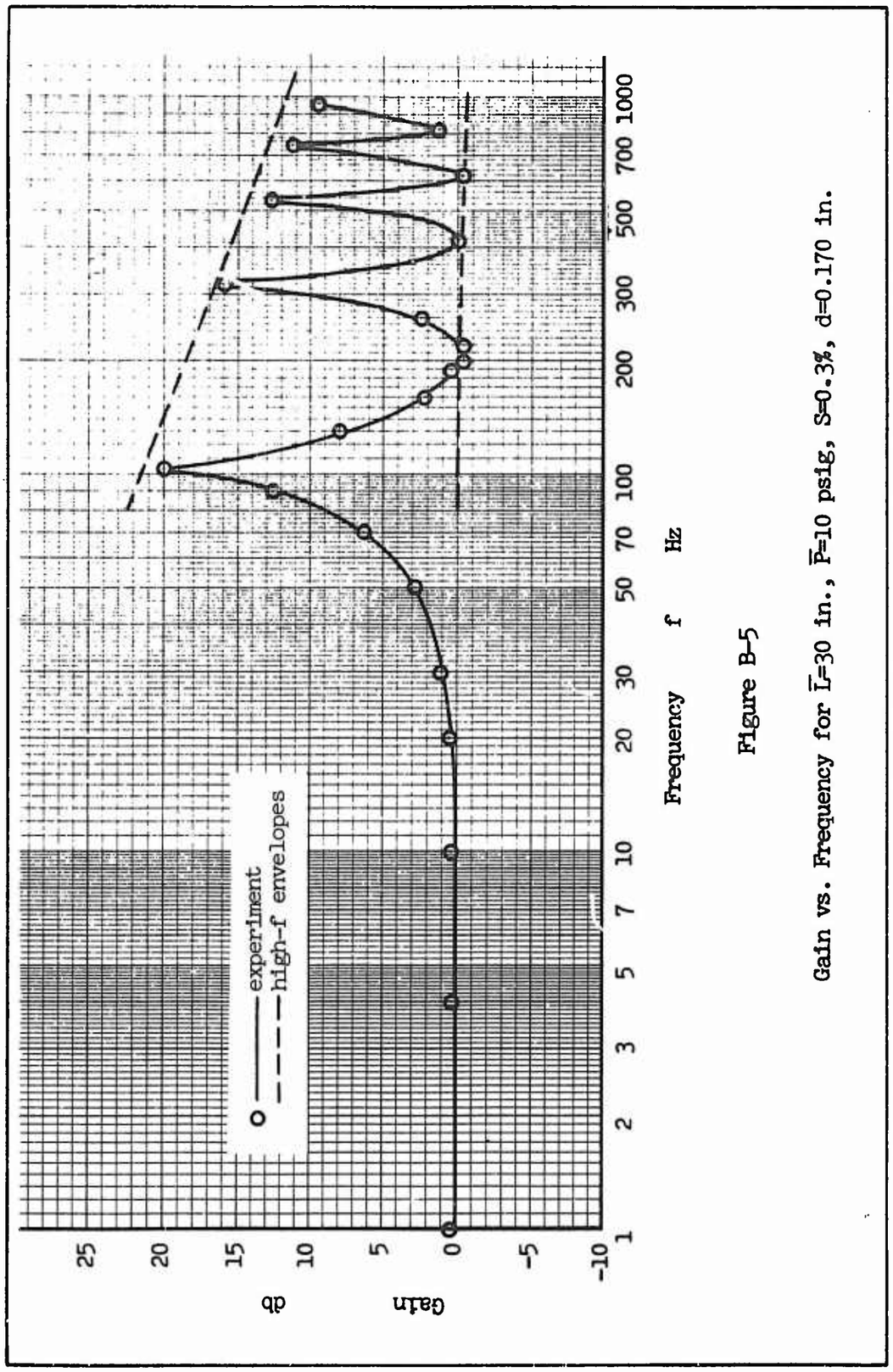

Figure B-5

Gain vs. Frequency for $\bar{L}$=30 in., $\bar{P}$=10 psig, S=0.3%, d=0.170 in.

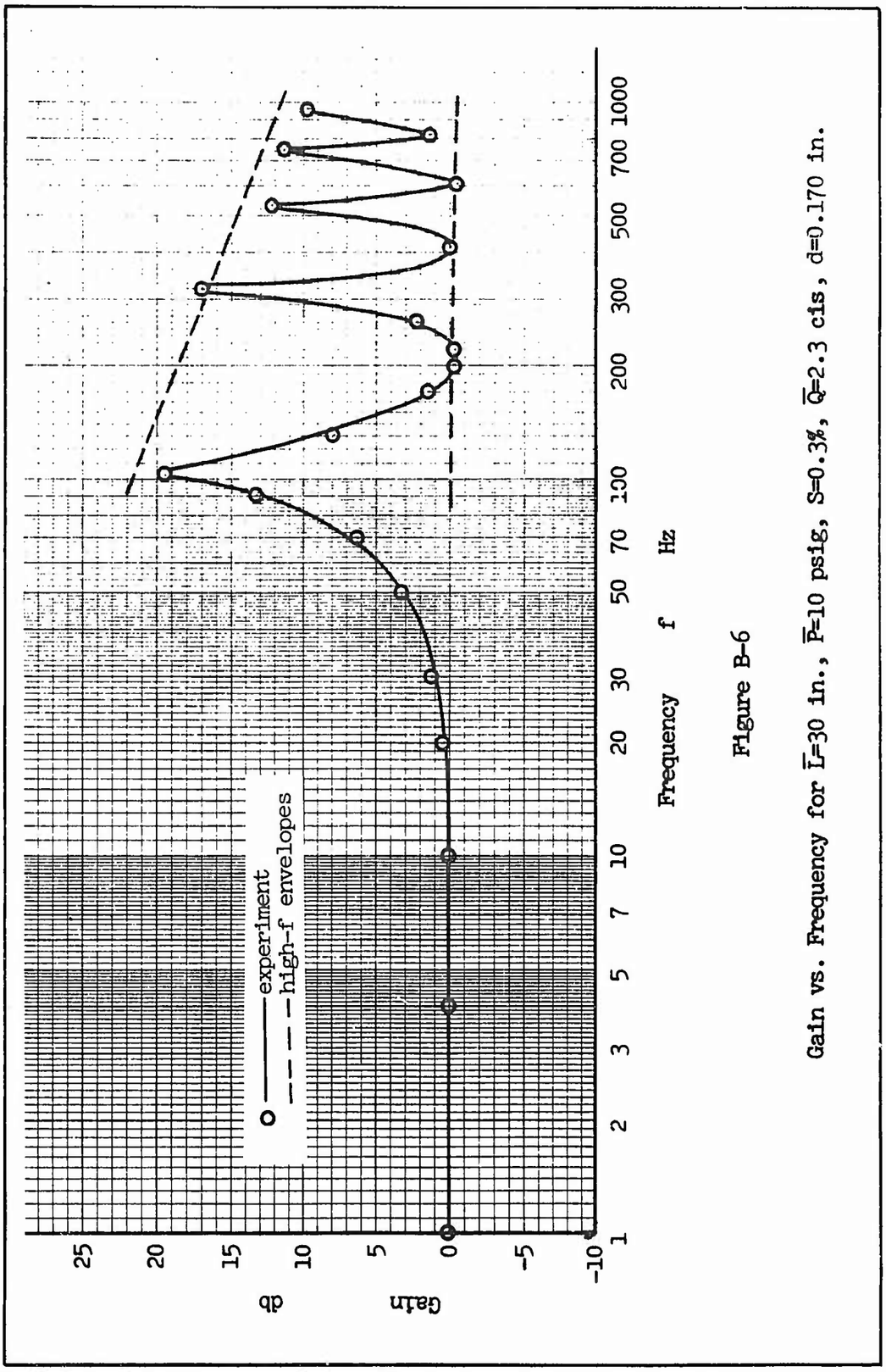

Figure B-6

Gain vs. Frequency for $\bar{L}$=30 in., $\bar{P}$=10 psig, S=0.3%, $\bar{Q}$=2.3 cis, d=0.170 in.

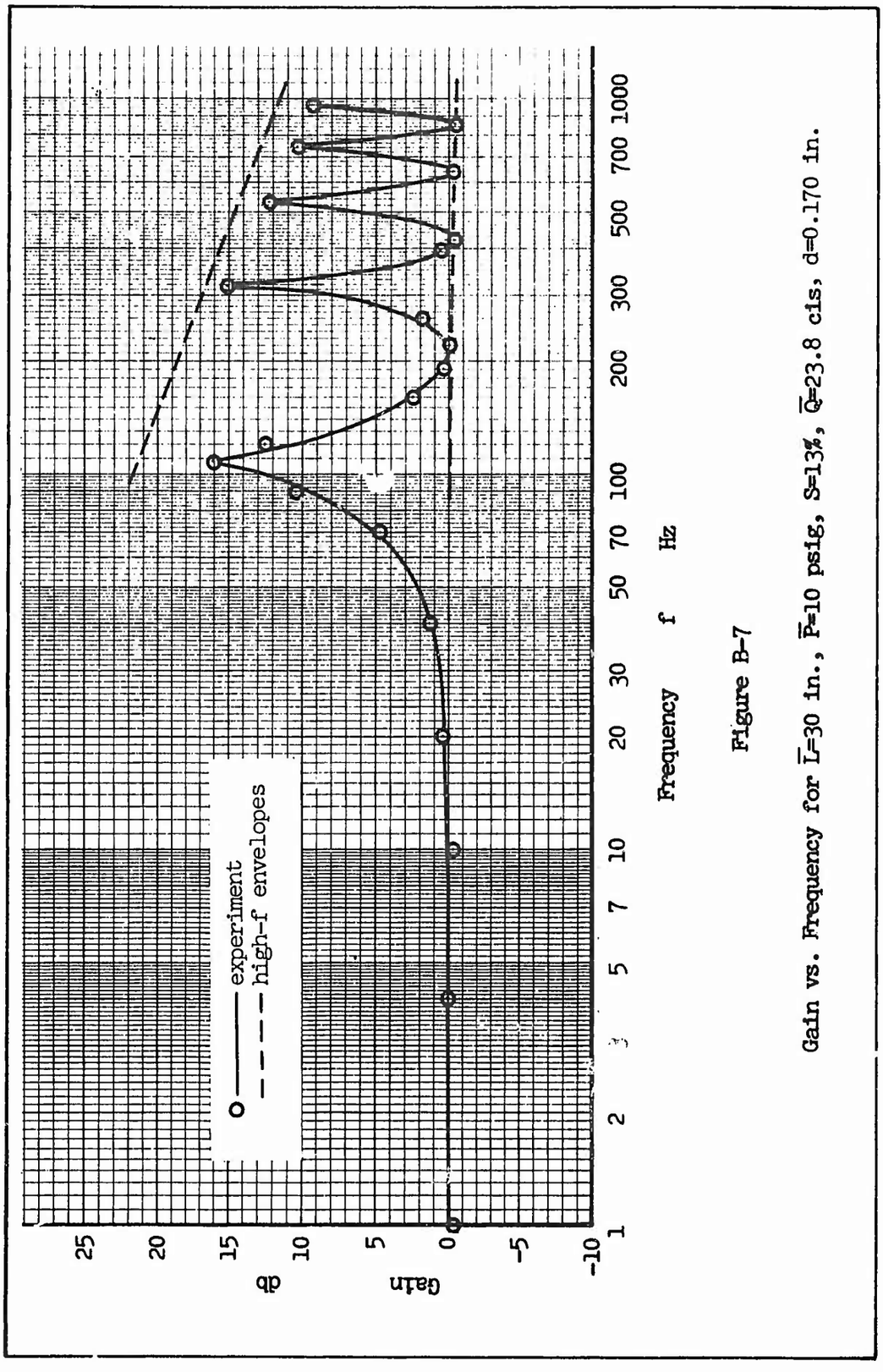

Figure B-7

Gain vs. Frequency for $\bar{L}$=30 in., $\bar{P}$=10 psig, S=13%, $\bar{Q}$=23.8 cis, d=0.170 in.

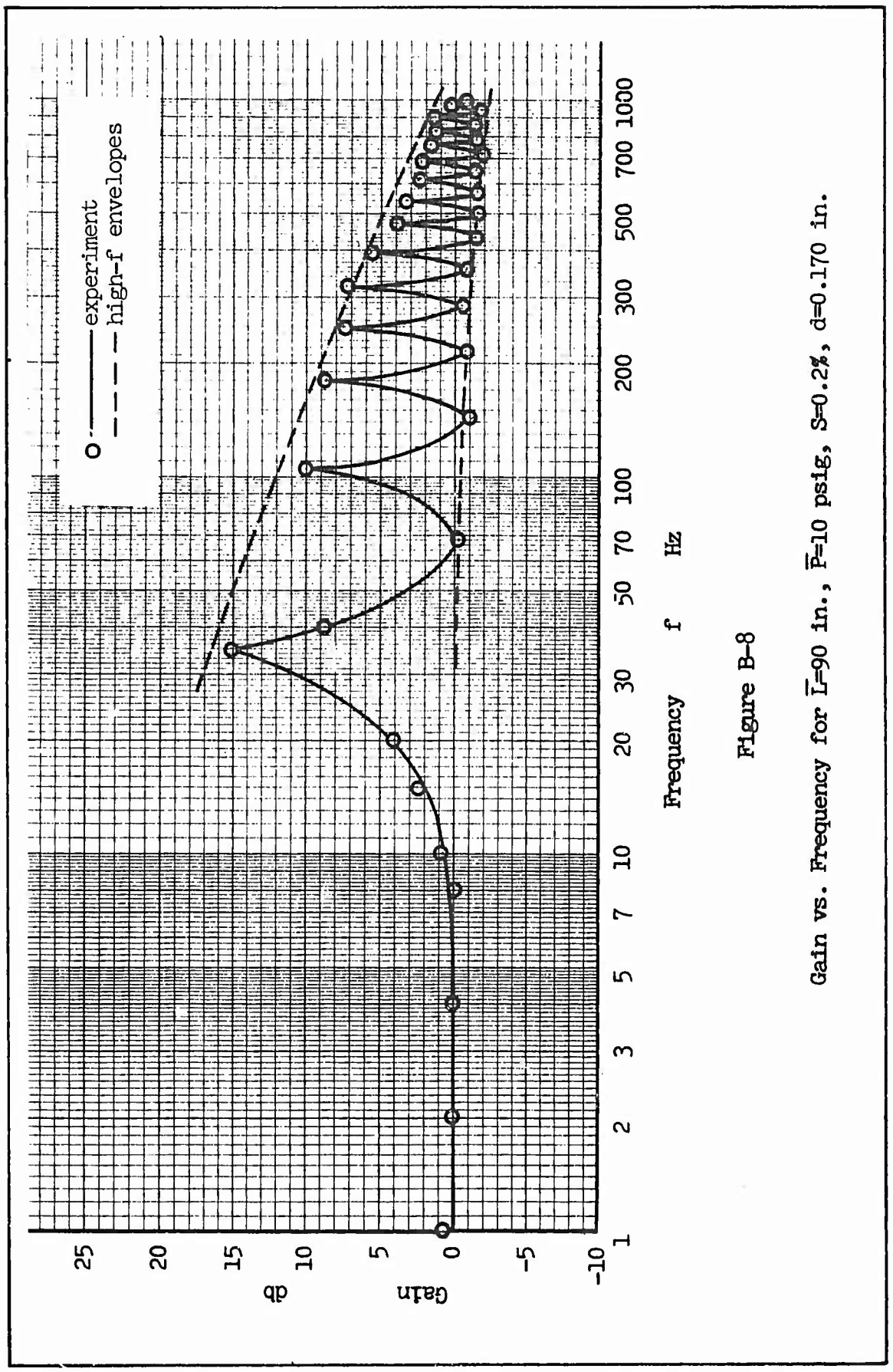

Figure B-8

Gain vs. Frequency for $\bar{L}$=90 in., $\bar{P}$=10 psig, S=0.2%, d=0.170 in.

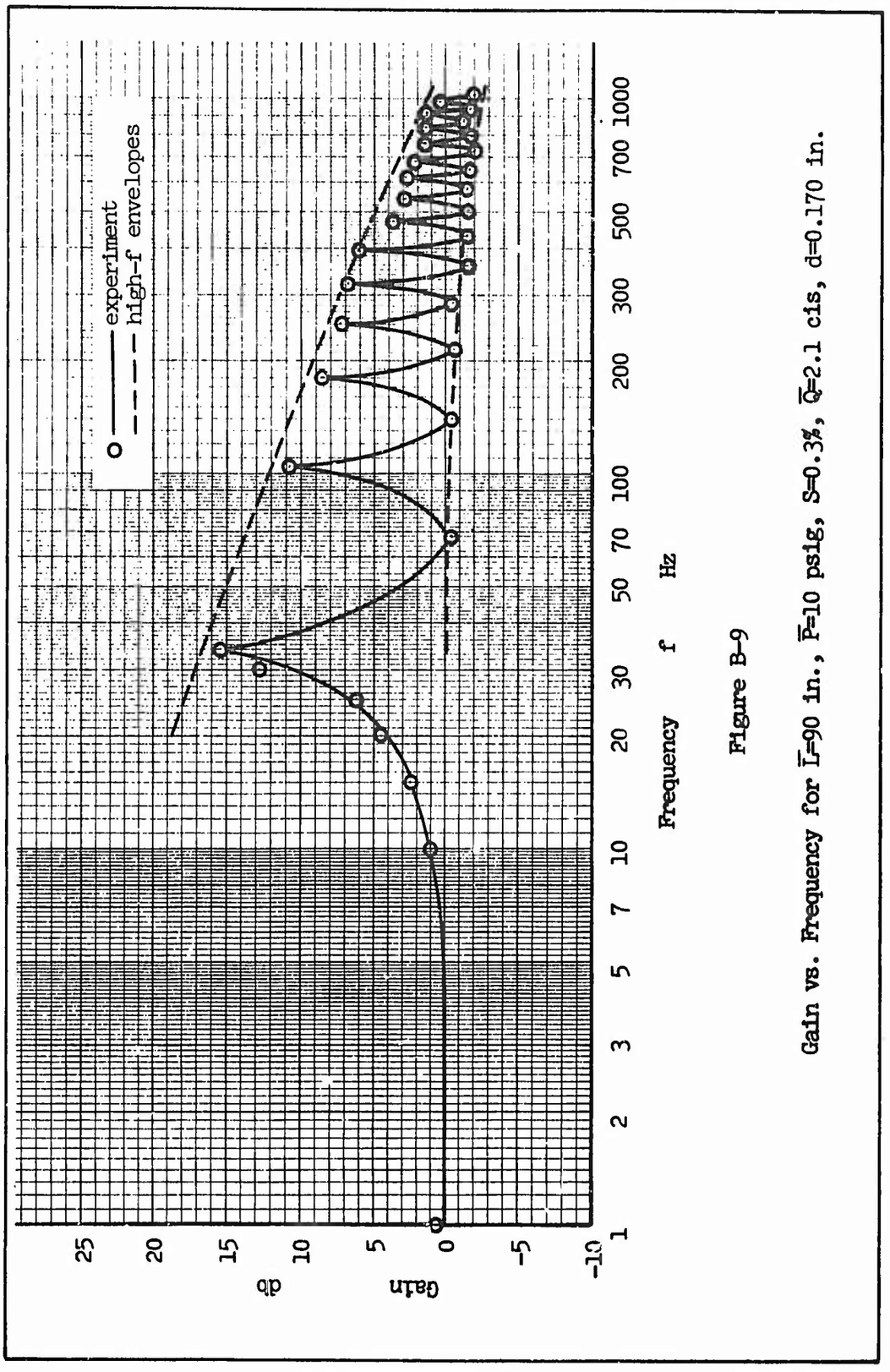

Figure B-9

Gain vs. Frequency for $\bar{L}$=90 in., $\bar{P}$=10 psig, S=0.3%, $\bar{Q}$=2.1 cis, d=0.170 in.

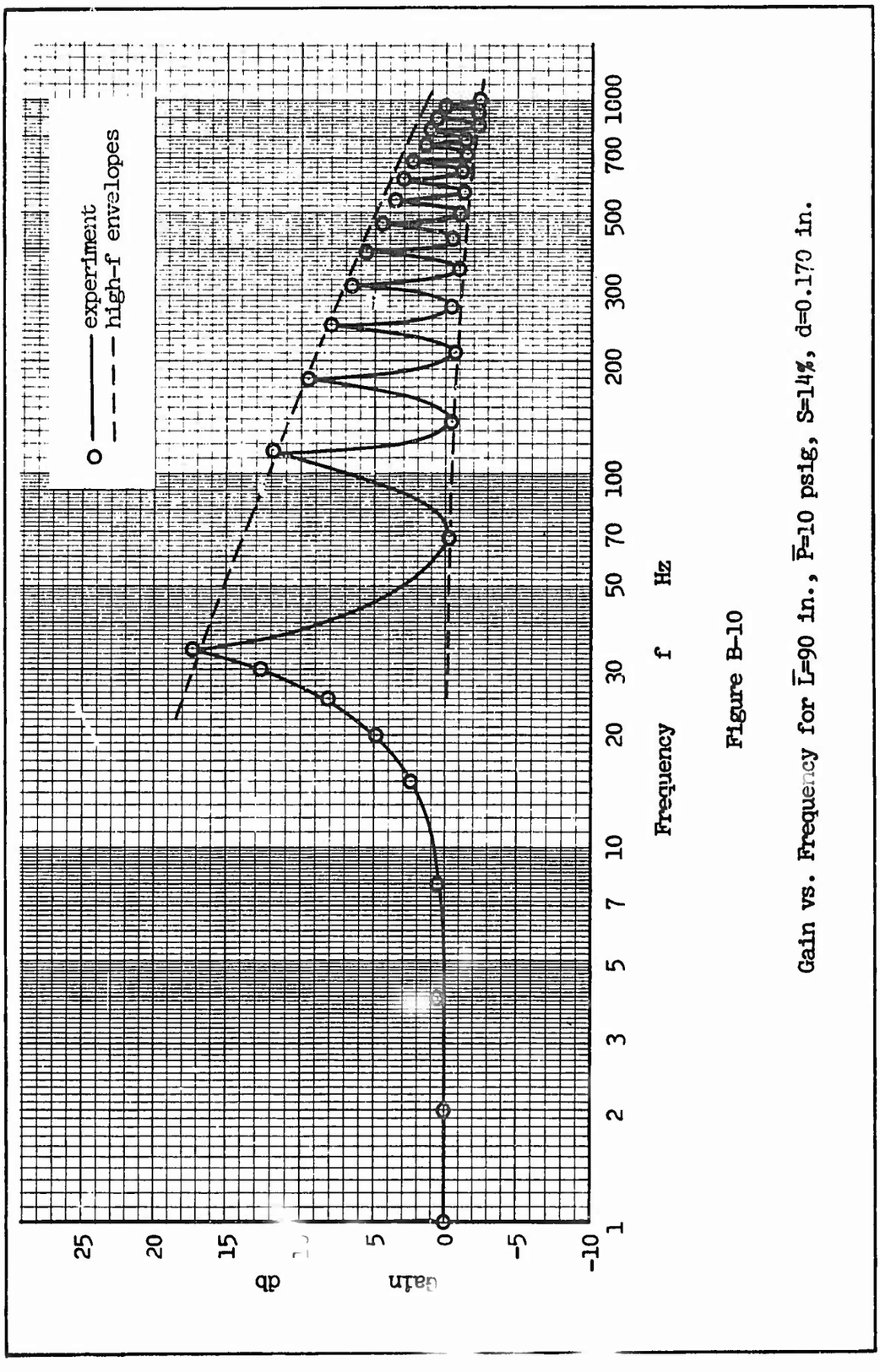

Figure B-10

Gain vs. Frequency for $\bar{L}$=90 in., $\bar{P}$=10 psig, S=14%, d=0.170 in.

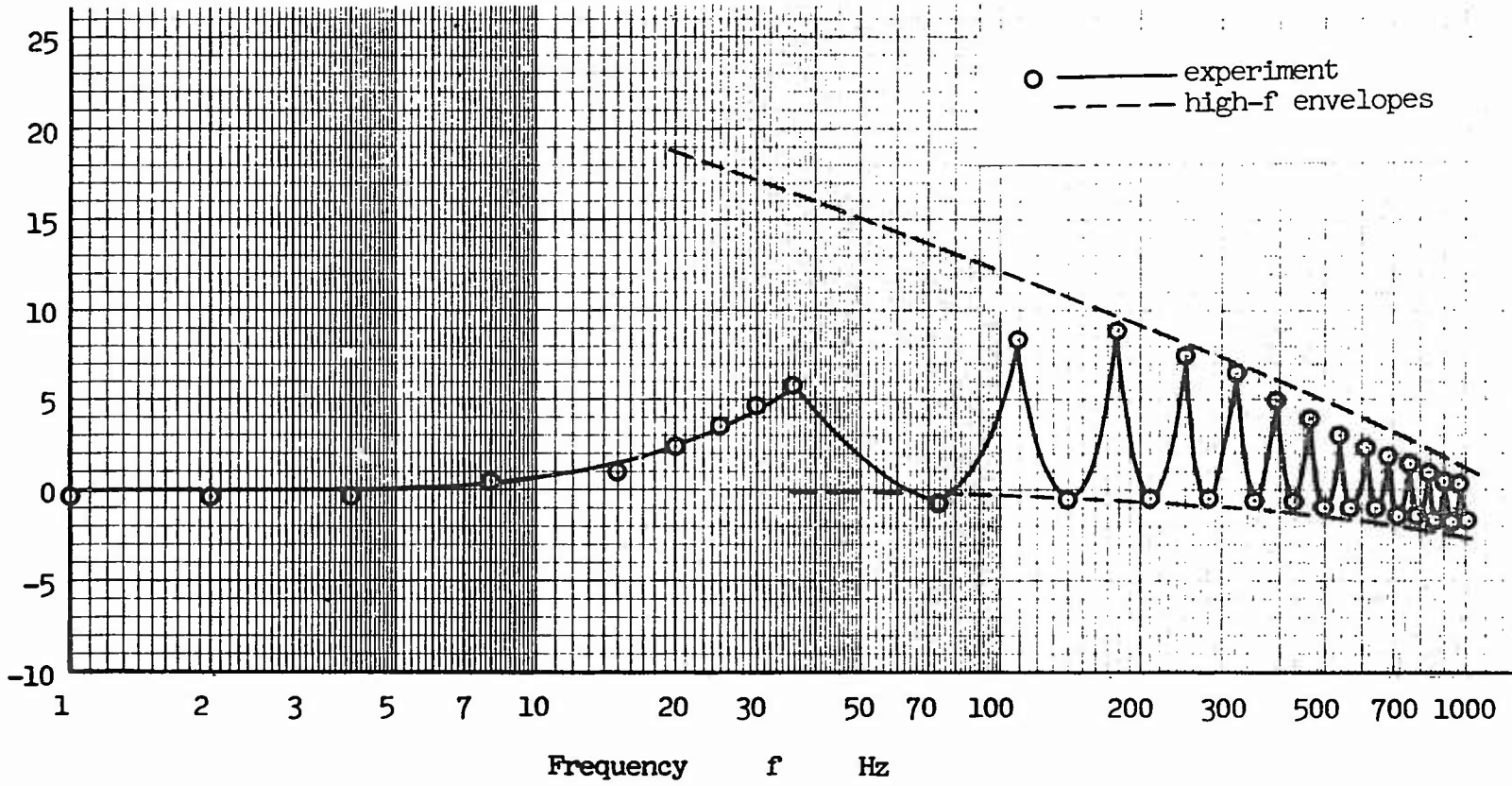

Figure B-11

Gain vs. Frequency for $\bar{L}$=90 in., $\bar{P}$=10 psig, S=13%, $\bar{Q}$=23.6 cis, d=0.170 in.

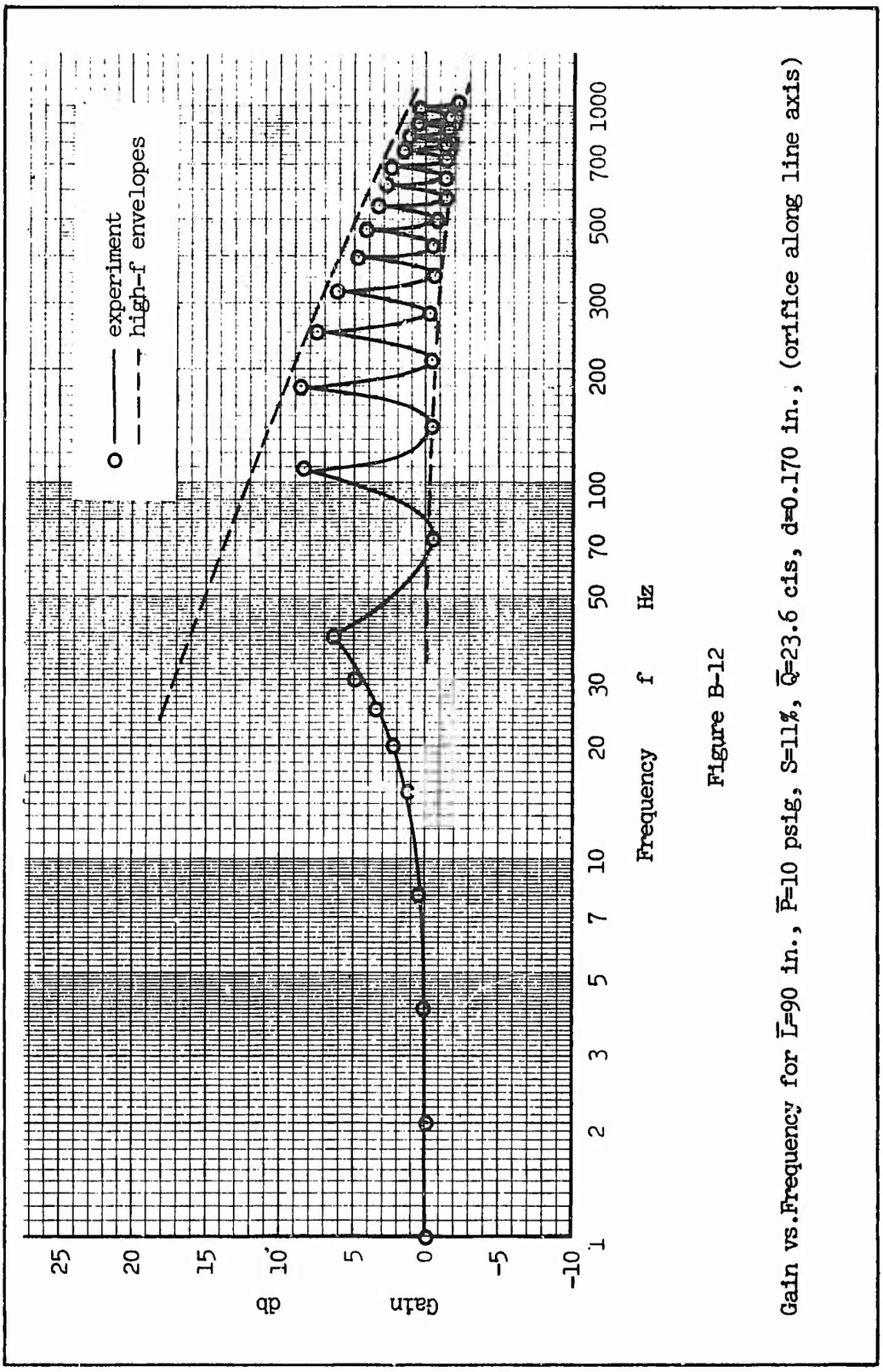

Figure B-12

Gain vs.Frequency for $\bar{L}$=90 in., $\bar{P}$=10 psig, S=11%, $\bar{Q}$=23.6 cis, d=0.170 in., (orifice along line axis)

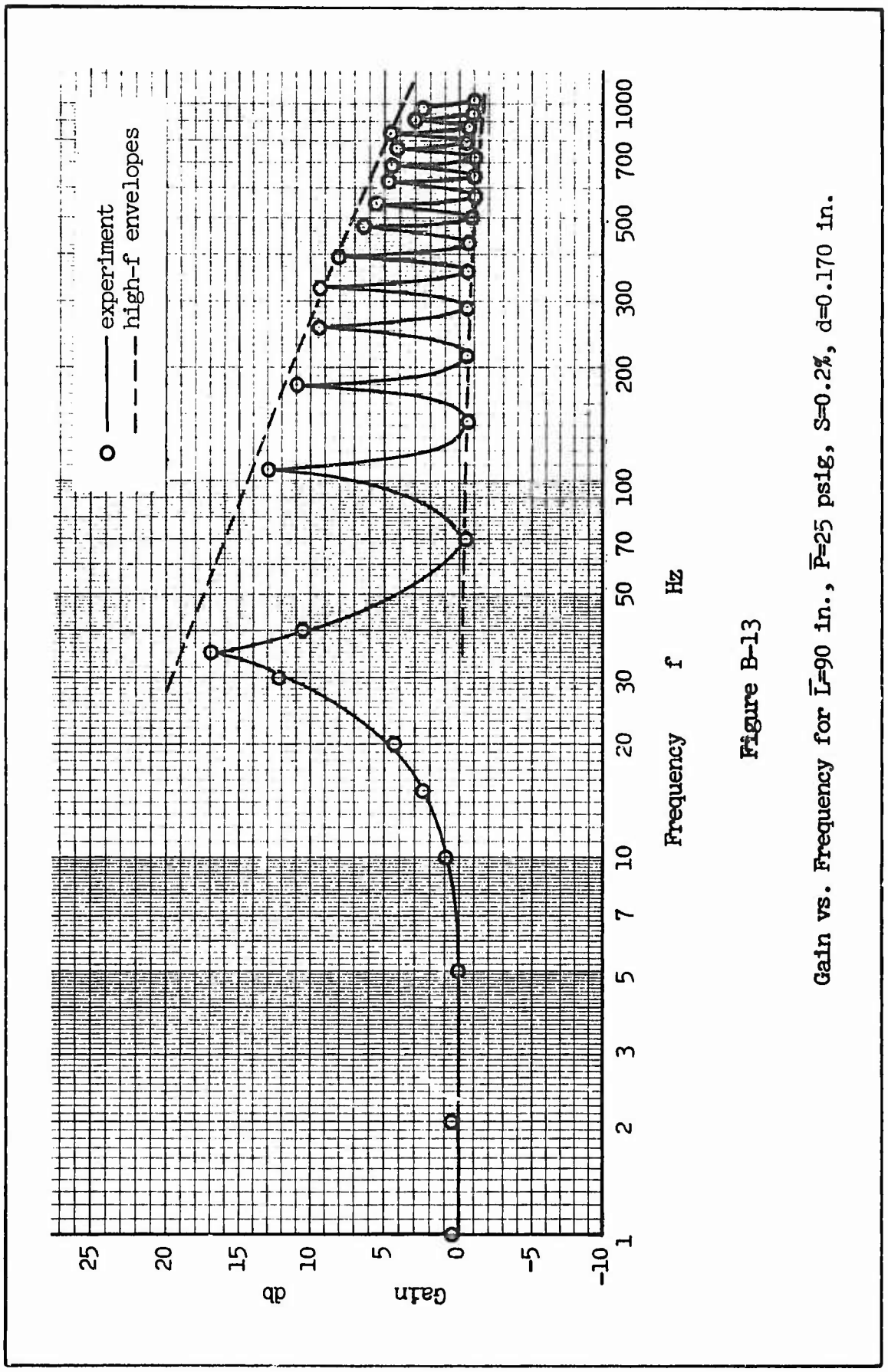

Figure B-13

Gain vs. Frequency for $\bar{L}$=90 in., $\bar{P}$=25 psig, S=0.2%, d=0.170 in.

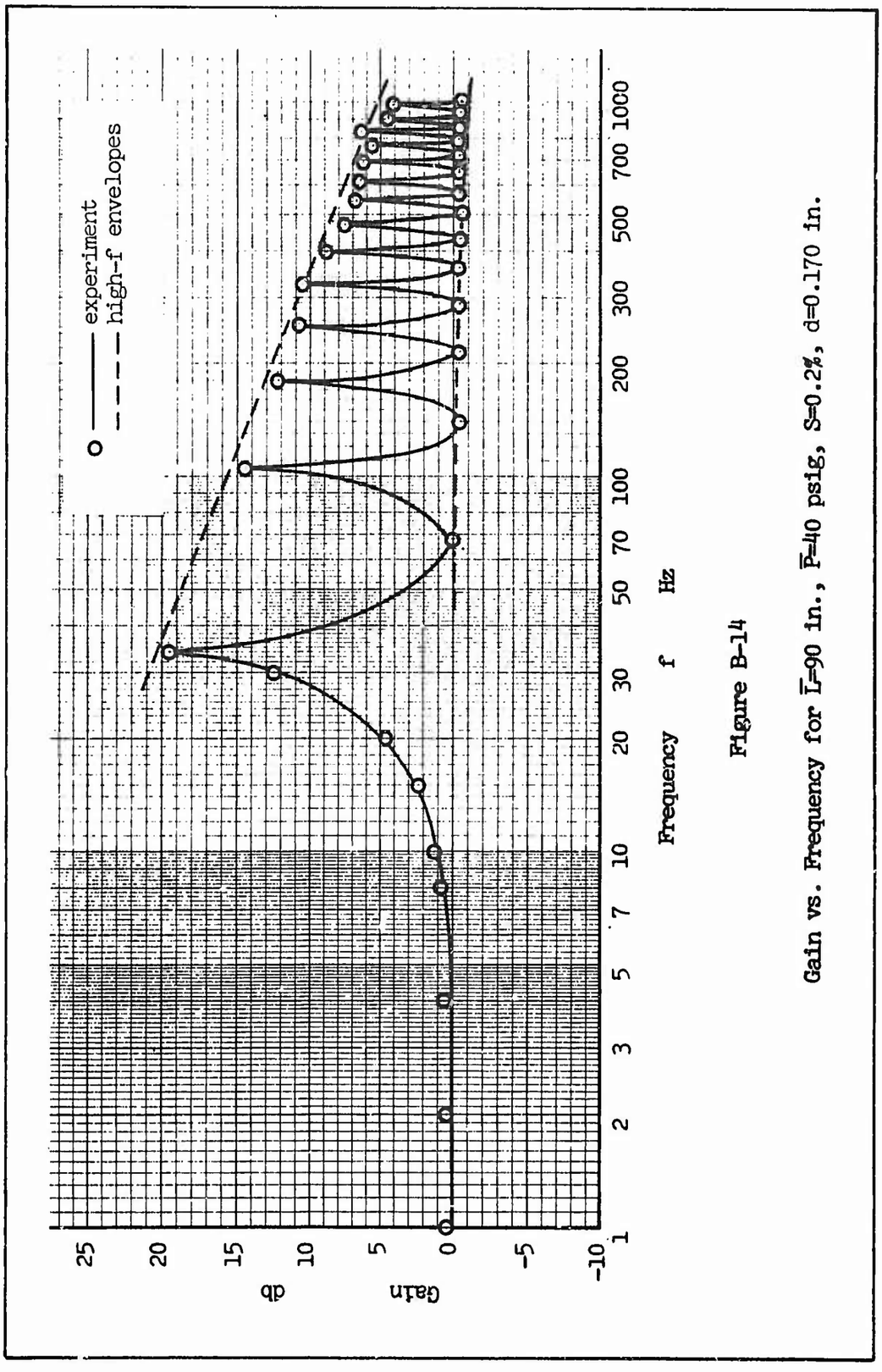

Figure B-14

Gain vs. Frequency for $\bar{L}$=90 in., $\bar{P}$=40 psig, S=0.2%, d=0.170 in.

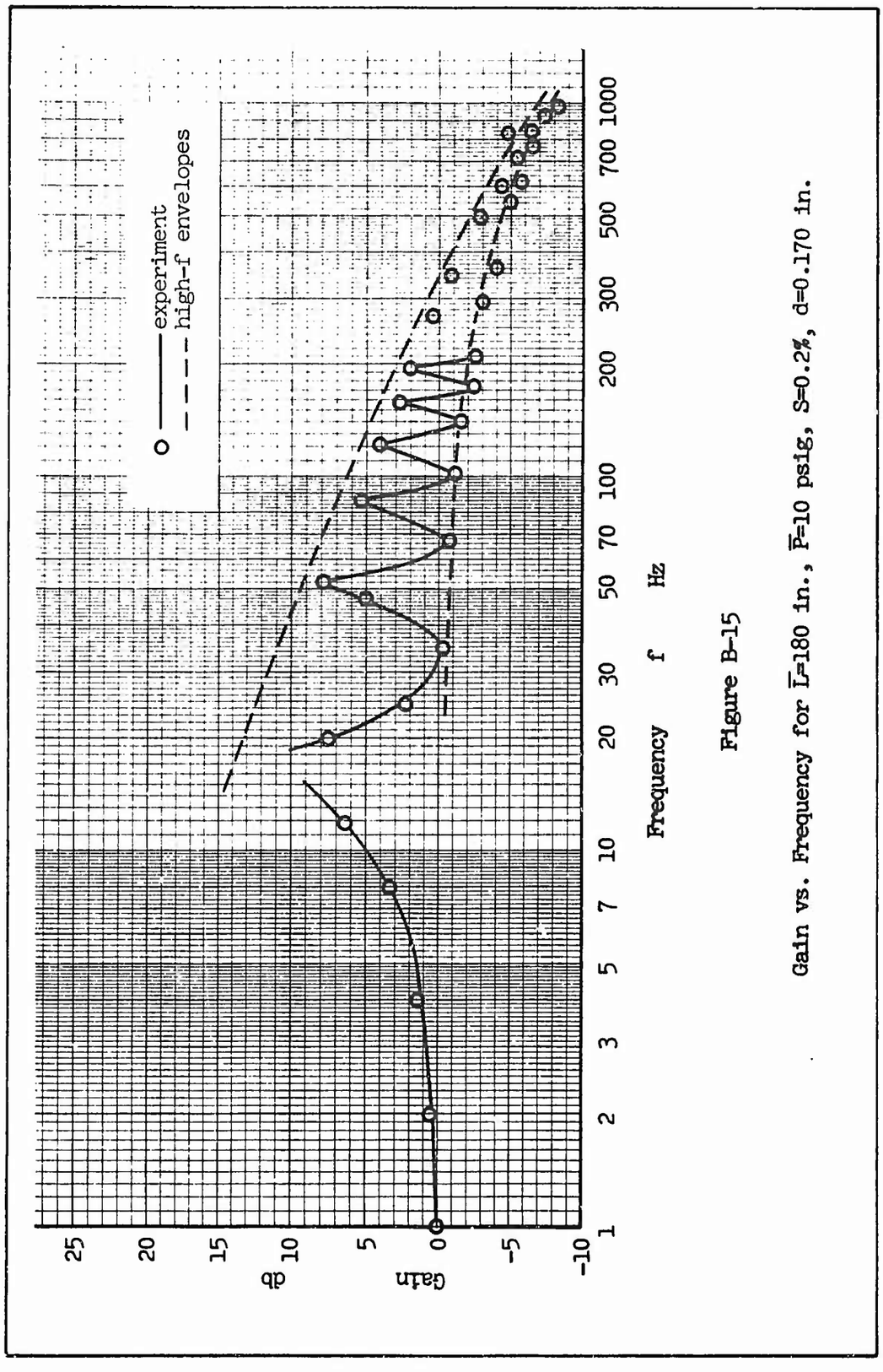

Figure B-15

Gain vs. Frequency for $\bar{L}$=180 in., $\bar{P}$=10 psig, S=0.2%, d=0.170 in.

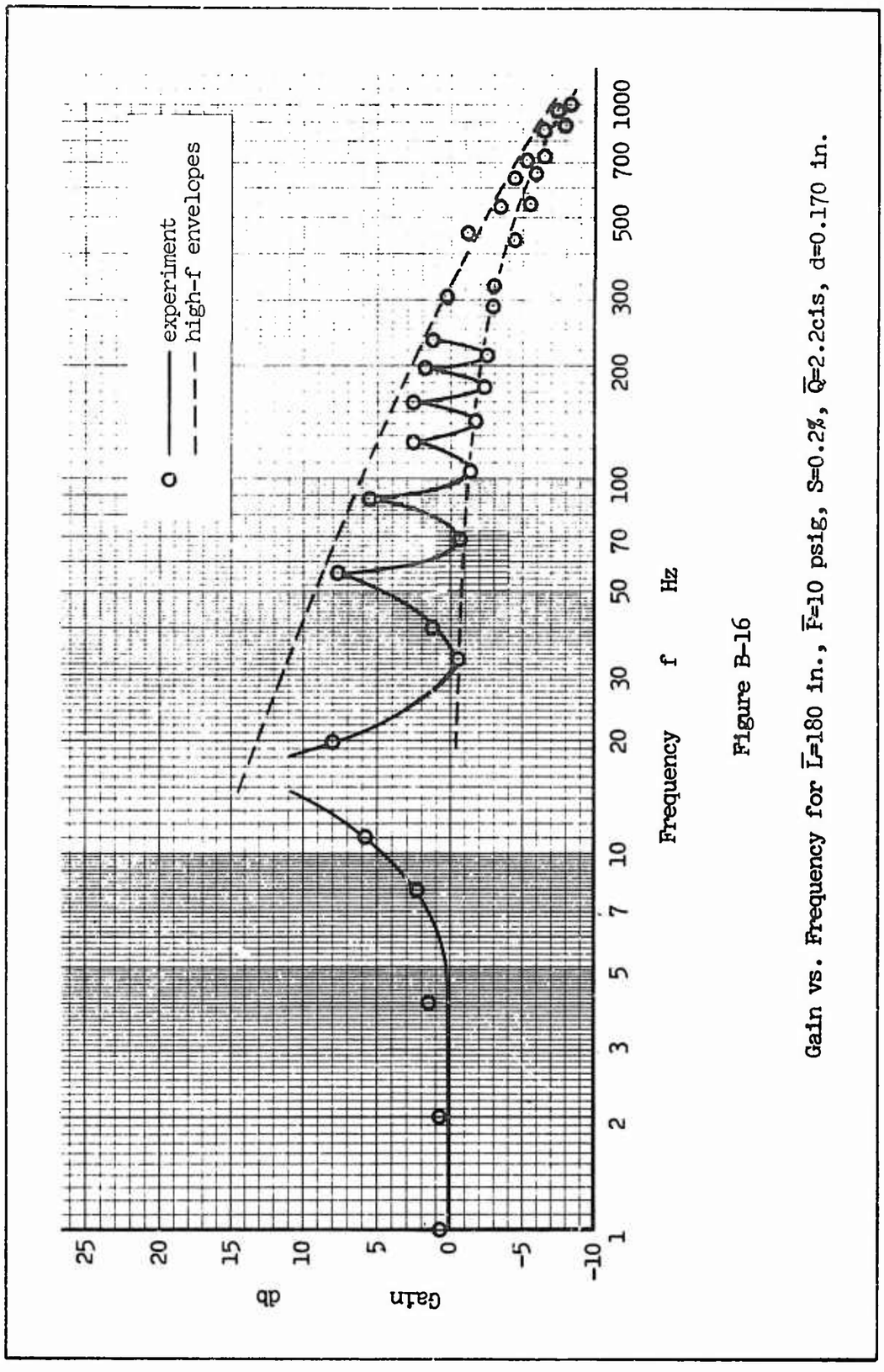

Figure B-16

Gain vs. Frequency for $\bar{L}$=180 in., $\bar{F}$=10 psig, S=0.2%, $\bar{Q}$=2.2cis, d=0.170 in.

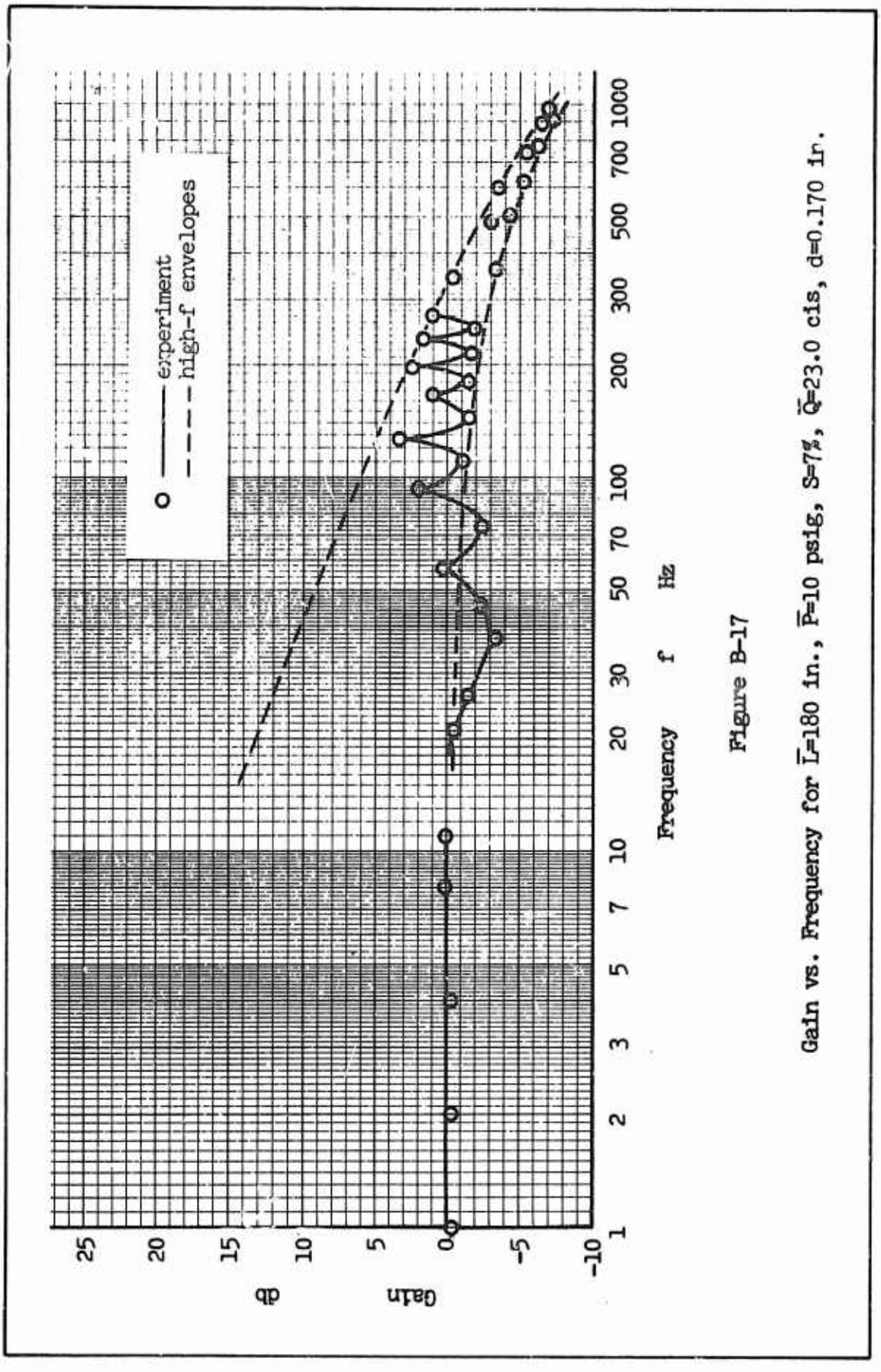

Figure B-17

Gain vs. Frequency for $\bar{L}$=180 in., $\bar{P}$=10 psig, S=7%, $\bar{Q}$=23.0 cis, d=0.170 in.

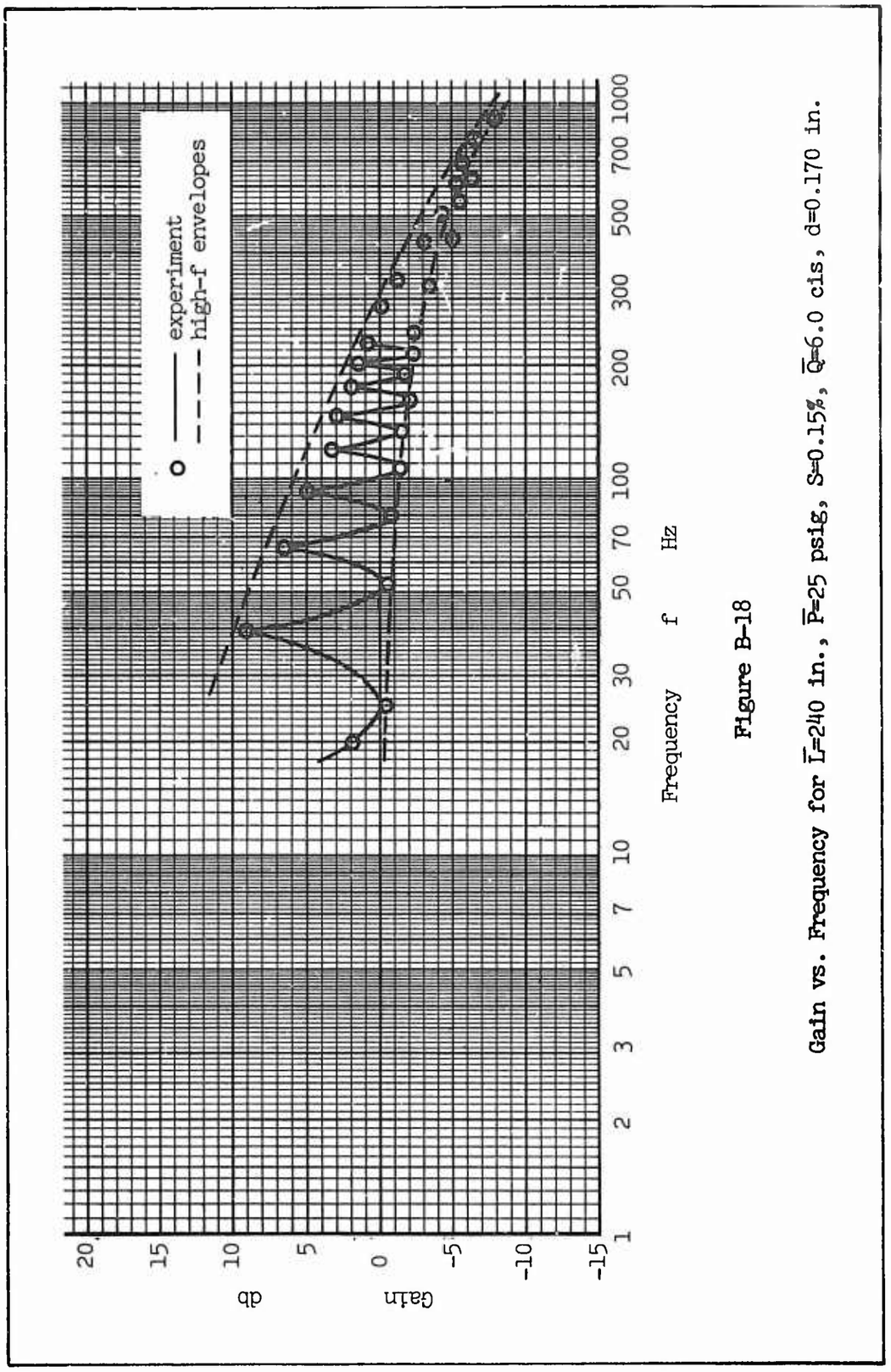

Figure B-18

Gain vs. Frequency for $\bar{L}$=240 in., $\bar{P}$=25 psig, S=0.15%, $\bar{Q}$=6.0 cis, d=0.170 in.

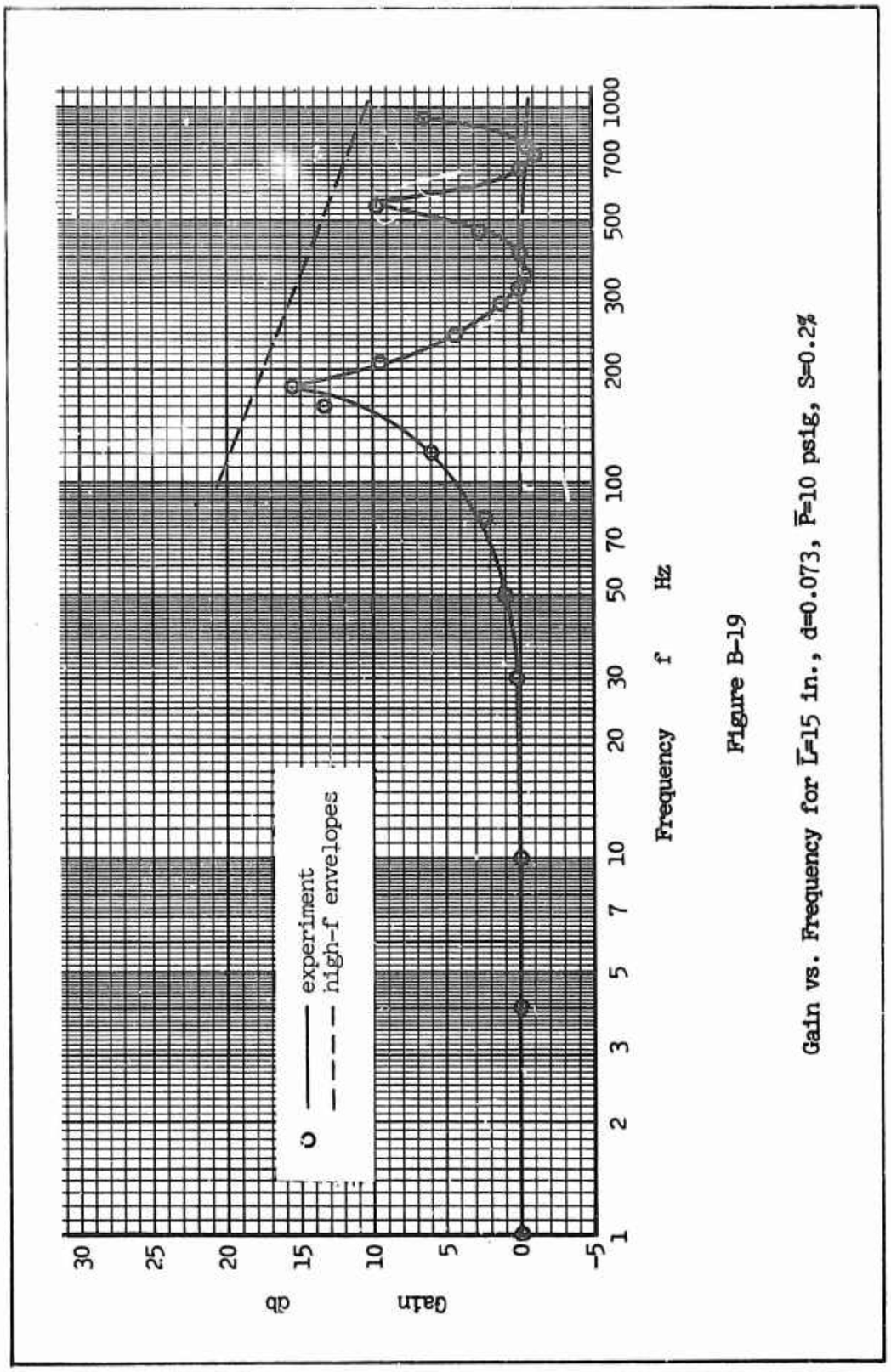

Figure B-19

Gain vs. Frequency for $\bar{L}$=15 in., d=0.073, $\bar{P}$=10 psig, S=0.2%

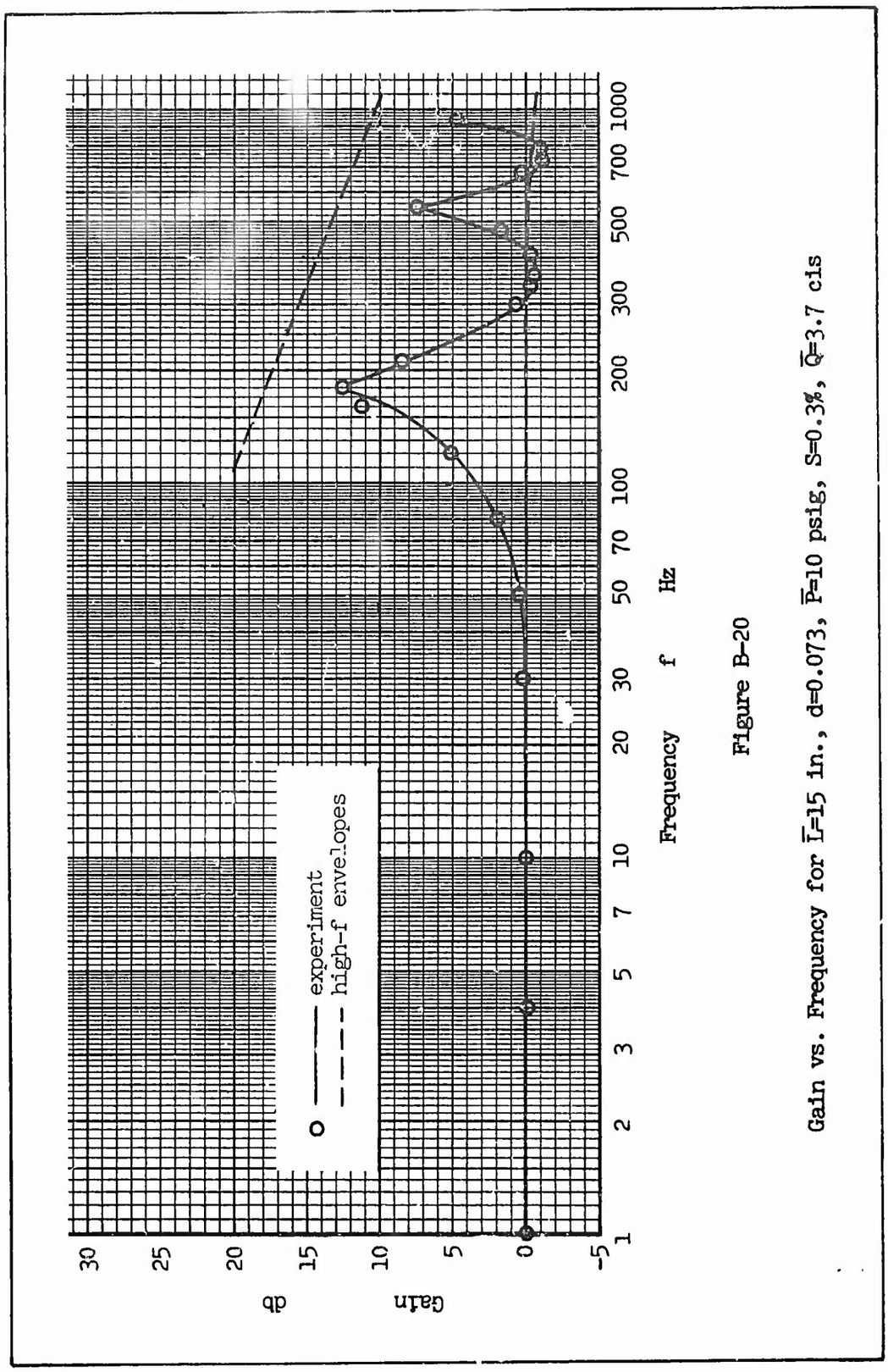

Figure B-20

Gain vs. Frequency for $\bar{L}$=15 in., d=0.073, $\bar{P}$=10 psig, S=0.3%, $\bar{Q}$=3.7 cis

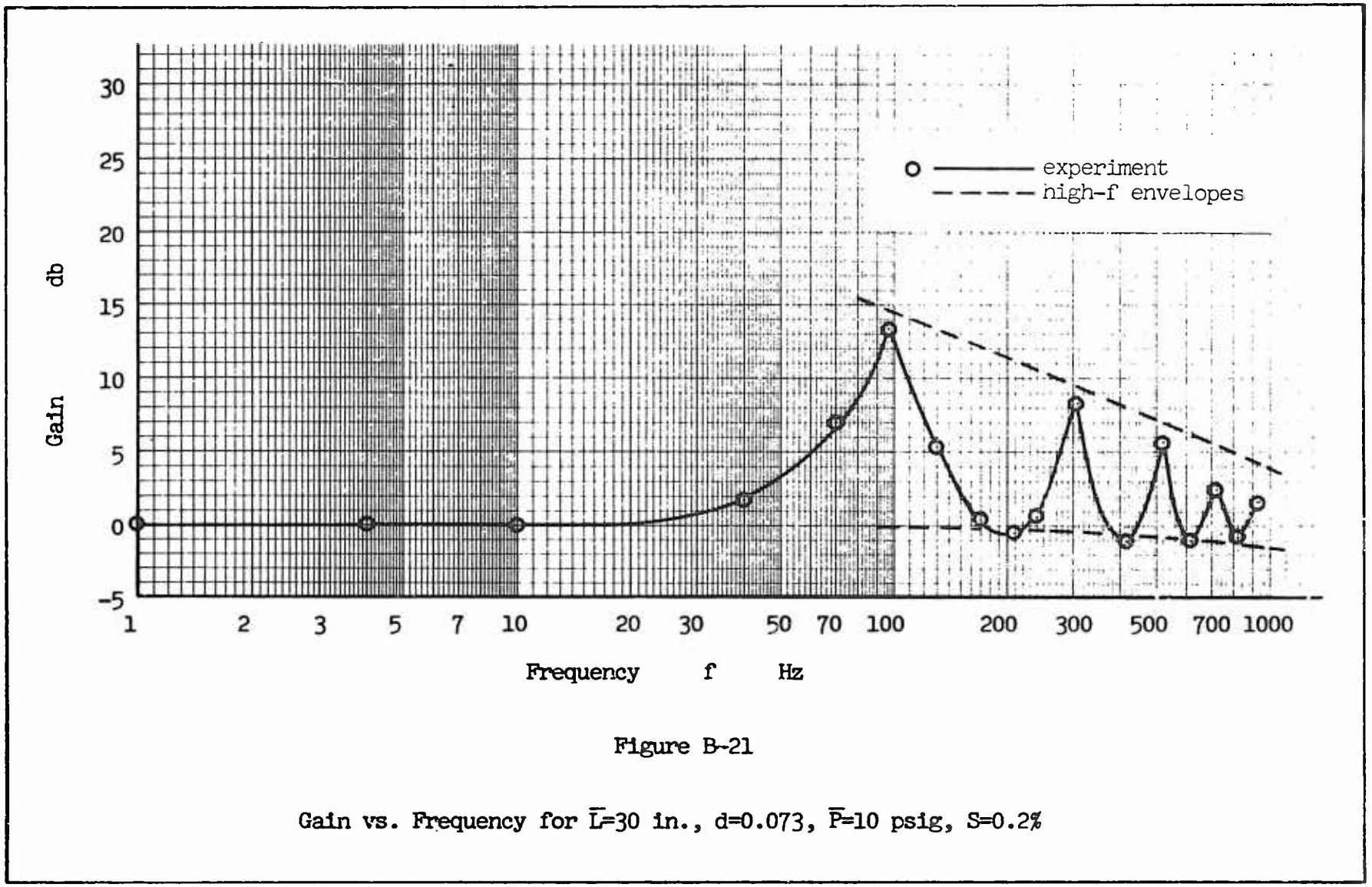

Figure B-21

Gain vs. Frequency for $\bar{L}$=30 in., d=0.073, $\bar{P}$=10 psig, S=0.2%

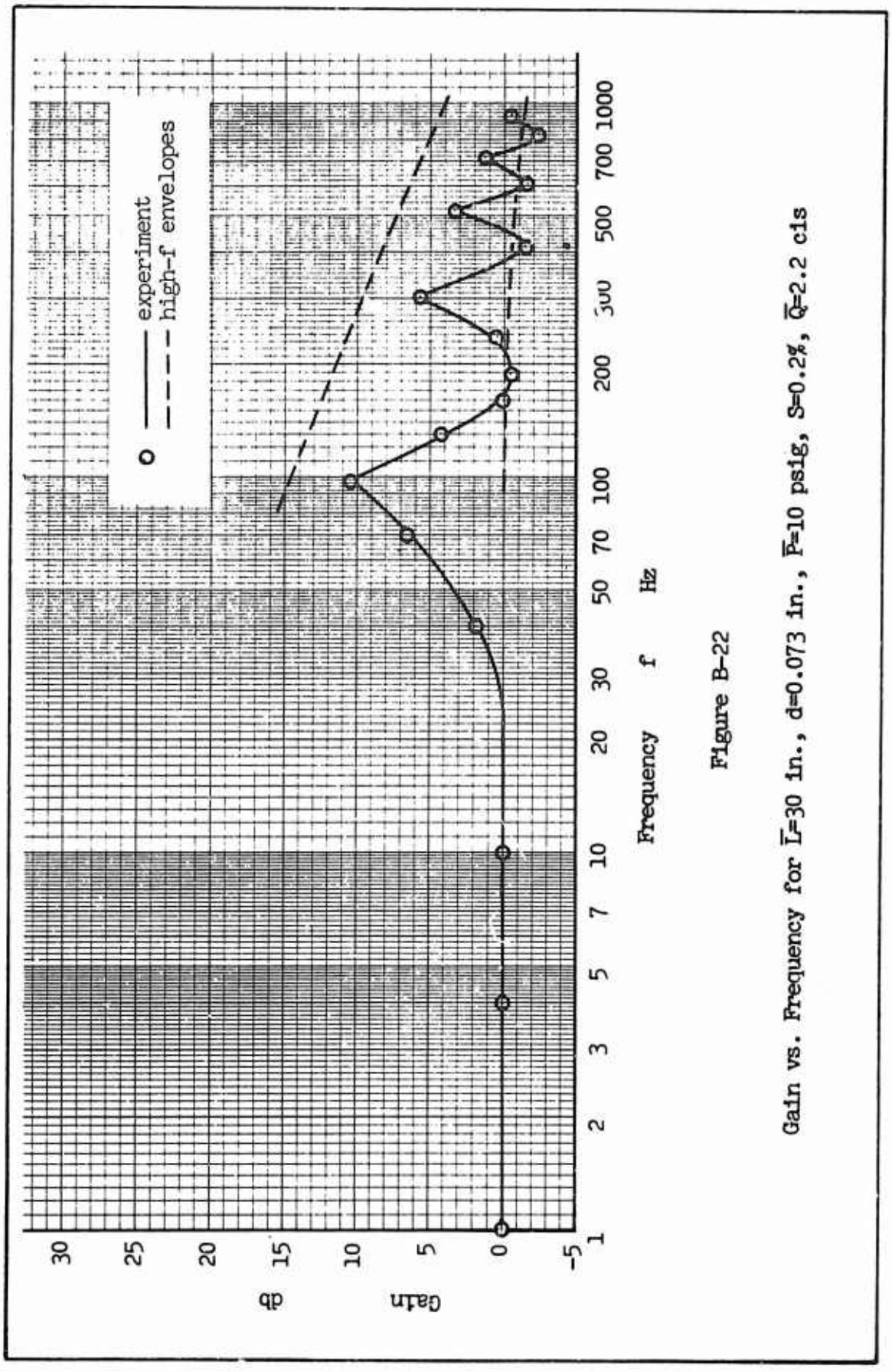

Figure B-22

Gain vs. Frequency for $\bar{L}$=30 in., d=0.073 in., $\bar{P}$=10 psig, S=0.2%, $\bar{Q}$=2.2 cis

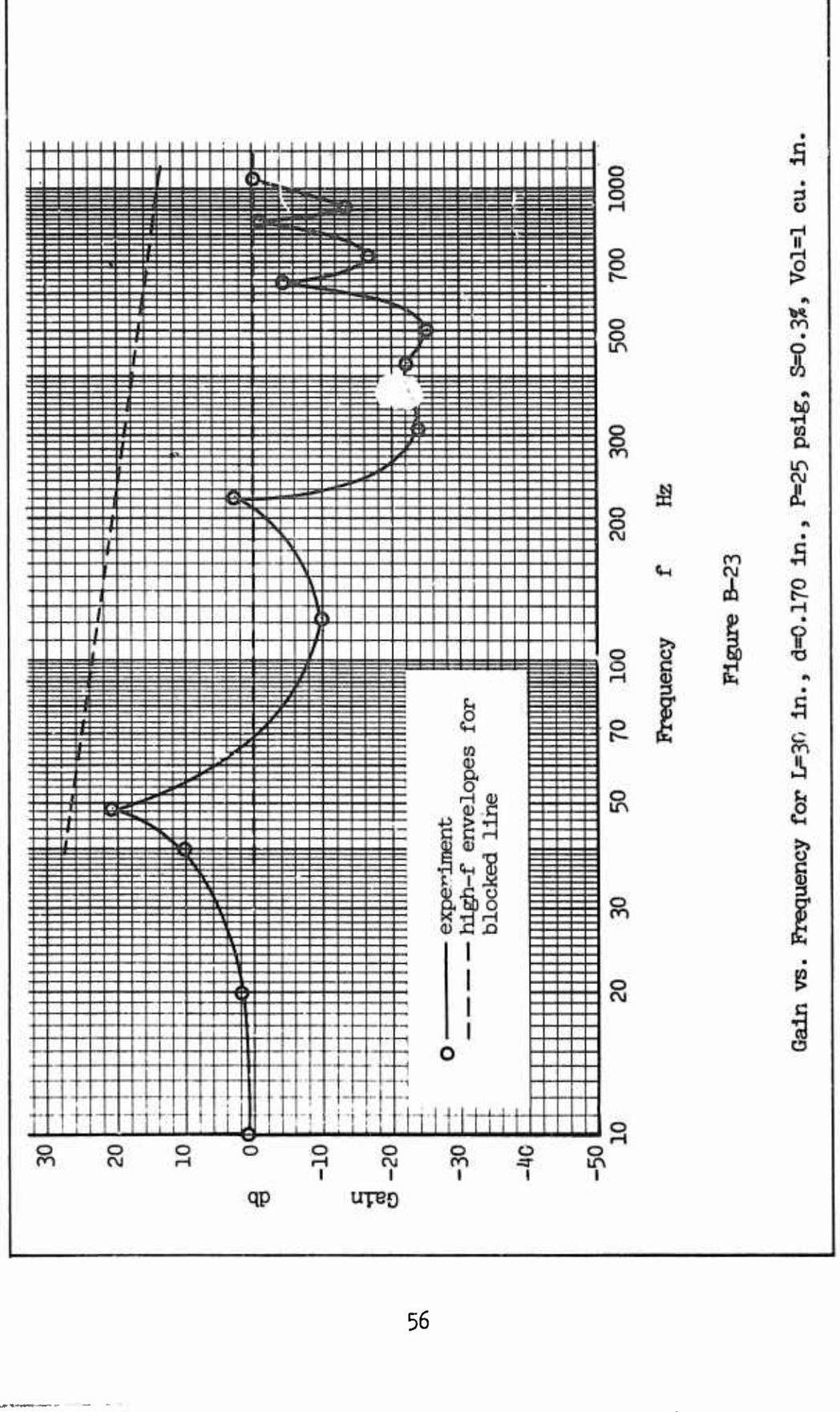

Figure B-23

Gain vs. Frequency for L=30 in., d=0.170 in., P=25 psig, S=0.3%, Vol=1 cu. in.

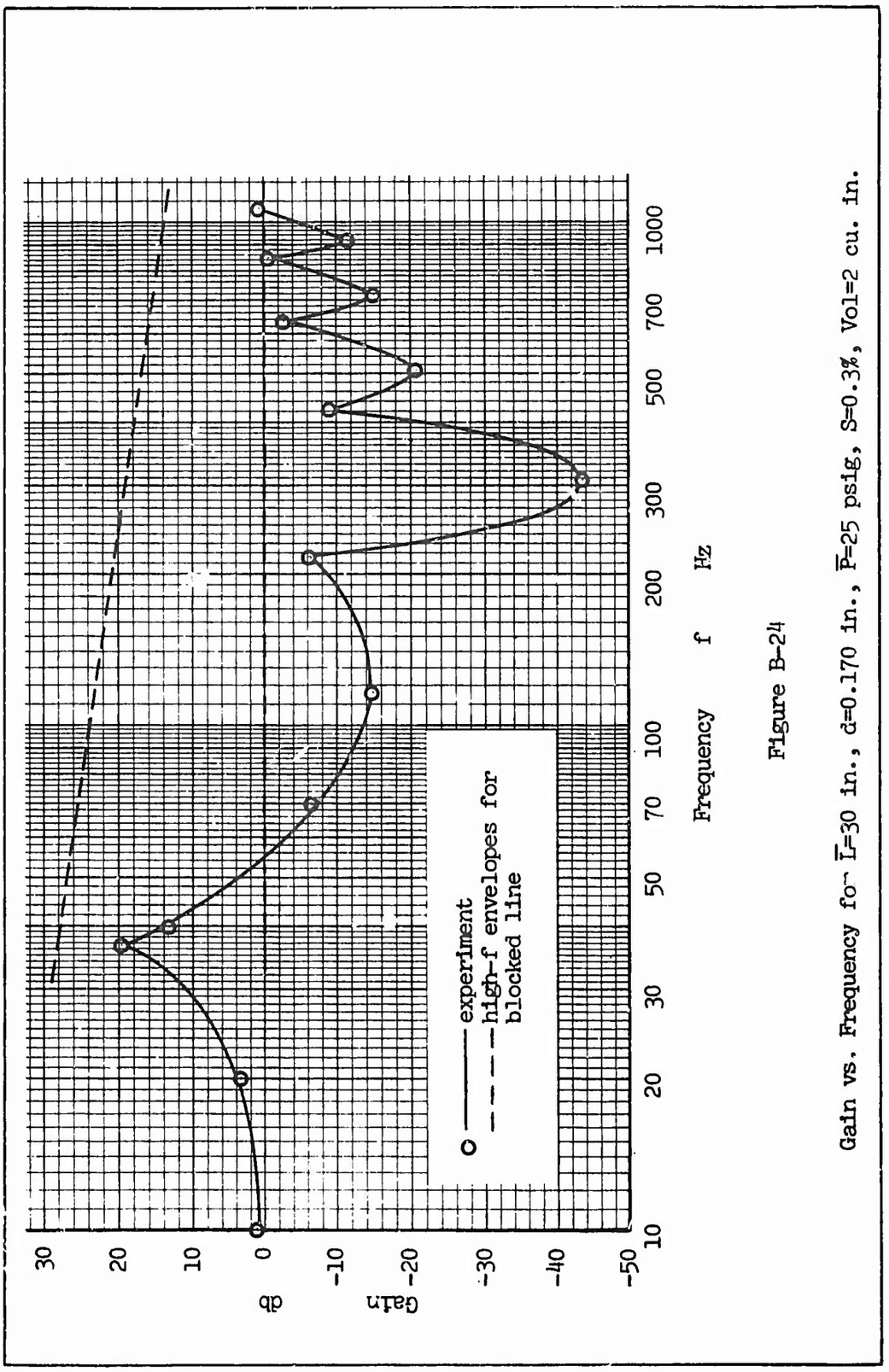

Figure B-24

Gain vs. Frequency for $\bar{L}$=30 in., d=0.170 in., $\bar{P}$=25 psig, S=0.3%, Vol=2 cu. in.

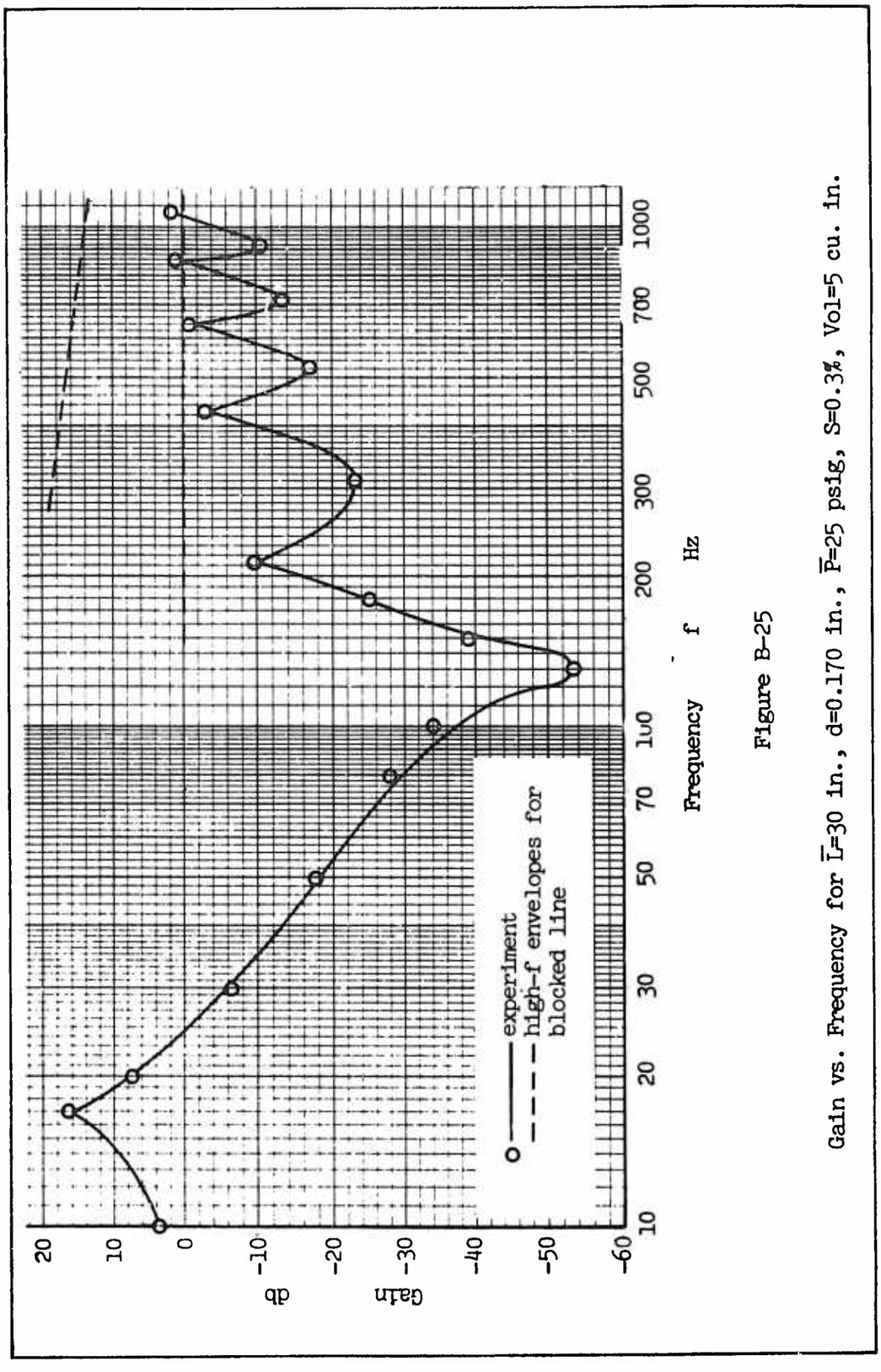

Figure B-25

Gain vs. Frequency for $\bar{L}$=30 in., d=0.170 in., $\bar{P}$=25 psig, S=0.3%, Vol=5 cu. in.

Table B-1

Data for $\overline{L}$ = 15 in, $\overline{P}$ = 10 psig, S = 0.2%, d_o = 0.020 in, $\overline{Q}$ = 3.7 cis, N_{Re} = 1910

f Hz	P_sx100 psi-rms	P_rx100 psi-rms	Gain db	f Hz	P_sx100 psi-rms	P_rx100 psi-rms	Gain db
1	2.25	2.25	0.0	400	2.55	2.55	0.0
3	1.95	2.06	0.3	416	2.30	2.25	-0.2
10	2.10	2.10	0.0	500	1.05	1.20	1.1
20	1.70	1.75	0.3	600	0.24	1.10	13.2
40	1.35	1.40	0.3	632	0.15	1.20	18.1
70	0.94	1.10	1.4	700	0.90	1.90	6.5
100	0.65	0.87	2.5	778	3.4	3.90	1.2
150	0.36	0.83	7.2	832	2.35	2.30	-0.2
200	0.076	0.78	20.2	900	1.50	1.55	0.3
208	0.065	0.79	21.7	950	0.46	2.35	14.2
300	0.82	1.30	3.0	1058	1.15	1.50	2.3
386	2.65	2.65	0.0				

Table B-2

Data for $\overline{L}$ = 15 in, $\overline{P}$ = 10 psig, S = 3.4%, d_o = 0.052 in, $\overline{Q}$ = 24.2 cis, N_{Re} = 12400

f Hz	P_sx100 psi-rms	P_rx100 psi-rms	Gain db	f Hz	P_sx100 psi-rms	P_rx100 psi-rms	Gain db
1	33.8	33.4	-0.1	400	14.5	15.0	0.3
4	31.2	31.0	0.0	416	11.0	11.0	0.0
10	24.4	24.4	0.0	446	7.9	7.9	0.0
20	16.5	16.5	0.0	474	6.1	6.5	0.5
40	9.8	10.0	0.2	500	5.0	5.9	1.4
70	5.7	6.4	1.0	600	1.75	5.9	10.6
100	4.0	5.3	2.4	637	1.05	5.9	15.0
150	2.05	4.4	6.6	700	5.6	12.0	6.6
200	0.55	4.3	17.9	761	17.0	21.0	1.9
209	0.39	4.4	21.1	833	10.5	10.5	0.0
250	1.50	5.1	10.6	880	8.0	8.0	0.0
300	4.9	7.7	3.9	950	5.9	7.5	2.1
373	18.5	19.5	0.4	1060	2.7	13.0	13.6

Table B-3

Data for $\overline{L}$ = 15 in, $\overline{P}$ = 25 psig, S = 0.15%, d_o = 0.020 in, $\overline{Q}$ = 6.1 cis, N_{Re} = 5020

f Hz	P_sx100 psi-rms	P_rx100 psi-rms	Gain db	f Hz	P_sx100 psi-rms	P_rx100 psi-rms	Gain db
1	3.74	3.74	0.0	386	4.4	4.6	0.4
4	3.33	3.44	0.3	416	4.0	4.0	0.0
10	3.24	3.33	0.1	500	1.75	2.0	1.1
20	2.75	2.75	0.0	600	0.47	1.75	11.4
30	2.25	2.30	0.1	636	0.21	1.90	19.2
40	2.05	2.15	0.4	700	1.35	3.01	6.9
70	1.65	1.90	1.2	779	6.11	7.0	1.2
100	1.00	1.40	2.9	832	4.11	4.0	-0.2
150	0.60	1.35	7.0	900	2.55	2.60	0.1
200	0.135	1.30	19.7	950	2.00	2.45	1.7
210	0.085	1.35	22.0	1000	1.40	2.60	5.4
300	1.25	2.0	4.1	1066	0.67	4.0	15.5

Table B-4

Data for $\overline{L}$ = 15 in, $\overline{P}$ = 40 psig, S = 0.15%, d_o = 0.020 in, $\overline{Q}$ = 8.3 cis, N_{Re} = 9840

f Hz	P_sx100 psi-rms	P_rx100 psi-rms	Gain db	f Hz	P_sx100 psi-rms	P_rx100 psi-rms	Gain db
1	5.1			280	1.10	2.20	6.0
4	4.42	4.61	0.3	340	3.20	3.90	1.7
10	4.5	4.5	0.0	420	5.00	5.00	0.0
20	3.6	3.6	0.0	500	2.20	2.55	1.3
40	2.80	2.90	0.3	600	0.64	2.25	10.9
70	2.20	2.45	0.9	639	0.25	2.50	20.0
120	1.20	1.95	4.2	700	1.60	3.80	7.5
180	0.40	1.70	12.6	782	7.80	9.0	1.2
200	0.17	1.75	20.3	860	4.2	4.1	-0.2
213	0.10	1.75	24.9	960	2.35	3.1	2.4
260	0.69	1.95	9.0	1071	0.79	5.3	16.5

Table B-5

Data for $\overline{L}$ = 30 in, $\overline{P}$ = 10 psig, S = 0.3%, d_o = 0.013 in

f Hz	P_sx100 psi-rms	P_rx100 psi-rms	Gain db	f Hz	P_sx100 psi-rms	P_rx100 psi-rms	Gain db
1	2.75	2.85	0.3	201	1.95	1.90	-0.3
4	2.69	2.75	0.2	220	1.75	1.70	-0.3
10	2.15	2.20	0.2	260	0.90	1.20	2.5
20	1.55	1.65	0.5	317	0.145	0.92	16.0
30	1.30	1.45	1.0	414	2.10	2.10	0.0
50	0.90	1.25	2.9	529	0.24	1.05	12.8
70	0.46	0.95	6.3	610	2.20	2.40	0.7
90	0.21	0.91	12.7	617	2.30	2.35	-0.2
103	0.10	1.00	20.0	745	0.33	1.20	11.2
130	0.46	1.15	8.0	818	2.45	2.85	1.29
160	1.10	1.40	2.1	954	0.50	1.50	9.50
190	1.85	1.90	0.3				

Table B-6

Data for $\overline{L}$ = 30 in, $\overline{P}$ = 10 psig, S = 0.3%, d_o = 0.013 in
$\overline{Q}$ = 2.3 cis, N_{Re} = 1150

f Hz	P_sx100 psi-rms	P_rx100 psi-rms	Gain db	f Hz	P_sx100 psi-rms	P_rx100 psi-rms	Gain db
1	2.56	2.56	0.0	201	1.80	1.78	-0.1
4	2.50	2.49	0.0	220	1.65	1.62	-0.2
10	2.13	2.15	0.0	260	0.85	1.10	2.2
20	1.52	1.60	0.3	317	0.12	0.86	17.1
30	1.28	1.40	1.0	412	1.90	1.90	0.0
50	0.83	1.20	3.2	531	0.23	0.94	12.2
70	0.44	0.90	6.2	613	2.10	2.20	0.4
90	0.19	0.87	13.2	747	0.31	1.15	11.4
102	0.10	0.96	19.6	818	2.20	2.60	1.4
130	0.44	1.10	8.0	959	0.48	1.50	9.9
170	1.20	1.42	1.4				

Table B-7

Data for $\overline{L}$ = 30 in, $\overline{P}$ = 10 psig, S = 13%, d_o = 0.052 in, $\overline{Q}$ = 23.9 cis, N_{Re} = 12150

f Hz	P_sx100 psi-rms	P_rx100 psi-rms	Gain db	f Hz	P_sx100 psi-rms	P_rx100 psi-rms	Gain db
1	130	128	-0.2	220	29.0	29.0	0.0
4	96.3	96.3	0.0	260	12.0	15.0	1.9
10	58.0	57.0	-0.2	318	2.45	14.0	15.1
20	32.0	33.0	0.3	397	38.0	41.0	0.7
40	17.0	19.5	1.3	420	28.5	28.0	-0.2
70	7.8	13.5	4.8	529	3.80	15.5	12.2
90	3.8	12.5	10.3	602	33.0	38.0	1.2
108	1.95	12.5	16.1	640	22.0	21.5	-0.2
120	3.0	13.0	12.7	744	5.6	18.5	10.3
160	15.7	21.0	2.5	809	31.0	38.0	1.8
190	45.0	47.0	0.3	850	22.6	22.0	-0.3
197	50.0	50.0	0.0	959	8.7	25.0	9.2

Table B-8

Data for L = 90 in, P = 10 psig, S = 0.2%, d_o = 0.013 in

f Hz	P_sx100 psi-rms	P_rx100 psi-rms	Gain db	f Hz	P_sx100 psi-rms	P_rx100 psi-rms	Gain db
1	2.16	2.36	0.7	393	0.42	0.80	5.8
2	2.14	2.14	0.0	430	1.40	1.20	-1.3
4	1.77	1.81	0.2	470	0.50	0.79	4.0
8	1.16	1.16	0.0	502	1.32	1.10	-1.6
10	1.02	1.12	0.8	540	0.54	0.78	3.2
15	0.59	0.79	2.5	572	1.35	1.15	-1.4
20	0.43	0.68	4.0	614	0.58	0.79	2.4
35	0.125	0.71	15.1	647	1.30	1.12	-1.3
40	0.26	0.72	8.8	687	0.63	0.81	2.2
68	1.41	1.38	-0.2	719	1.40	1.13	-1.9
104	0.25	0.79	10.0	760	0.71	0.87	1.8
142	1.59	1.40	-1.1	791	1.42	1.22	-1.3
180	0.26	0.72	8.8	829	0.77	0.91	1.4
214	1.16	1.07	-0.7	863	1.48	1.27	-1.3
250	0.30	0.71	7.5	905	0.87	1.02	1.4
286	1.15	1.10	-0.4	937	1.57	1.28	-1.8
322	0.31	0.72	7.3	976	0.97	1.02	0.2
357	1.20	1.10	-0.8	1000	1.52	1.39	-0.8

Table B-9

Data for $\overline{L}$ = 90 in, $\overline{P}$ = 10 psig, S = 0.3%, d_o = 0.013 in, $\overline{Q}$ = 2.1 cis, N_{Re} = 1060

f Hz	P_sx100 psi-rms	P_rx100 psi-rms	Gain db	f Hz	P_sx100 psi-rms	P_rx100 psi-rms	Gain db
1	2.55	2.74	0.6	468	0.53	0.82	3.8
10	1.25	1.40	1.0	505	1.40	1.15	-1.7
15	0.77	1.00	2.5	540	0.59	0.82	2.9
20	0.46	0.78	4.6	575	1.45	1.20	-1.6
25	0.35	0.77	6.1	617	0.62	0.87	2.9
30	0.18	0.80	12.9	650	1.40	1.15	-1.7
34	0.145	0.85	15.4	689	0.69	0.88	2.1
68	1.65	1.60	-0.3	724	1.45	1.15	-2.0
104	0.24	0.83	10.8	761	0.77	0.92	1.5
140	1.45	1.40	-0.3	795	1.50	1.20	-1.9
179	0.31	0.84	8.7	835	0.82	0.97	1.4
214	1.35	1.25	-0.6	845	0.78	1.15	3.3
251	0.35	0.80	7.2	867	1.50	1.30	-1.2
286	1.30	1.20	-0.7	907	0.90	1.05	1.3
321	0.36	0.80	6.9	940	1.60	1.30	-1.8
357	1.35	1.15	-1.4	979	1.00	1.05	0.4
395	0.40	0.81	6.1	1012	1.70	1.35	-2.0
431	1.40	1.20	-1.3				

Table B-10

Data for $\overline{L}$ = 90 in, $\overline{P}$ = 10 psig, S = 14%, d_o = 0.052 in

f Hz	P_sx100 psi-rms	P_rx100 psi-rms	Gain db	f Hz	P_sx100 psi-rms	P_rx100 psi-rms	Gain db
1	136.3	136.3	0.0	396	8.6	16.5	5.7
2	97.0	97.0	0.0	427	28.5	26.5	-0.6
4	55.5	57.0	0.3	468	10.0	17.0	4.6
8	34.8	35.4	0.2	500	30.0	26.5	-1.1
15	17.5	23.0	2.3	539	12.0	18.0	3.5
20	10.5	18.5	4.9	571	30.0	26.0	-1.2
25	6.7	17.0	8.1	615	13.5	19.0	3.0
30	3.8	16.5	12.7	644	29.5	26.0	-1.1
34	2.2	16.0	17.2	687	15.0	19.5	2.3
68	49.0	48.0	-0.2	717	30.0	25.0	-1.6
105	3.8	15.0	11.9	759	16.5	19.5	1.4
138	37.0	35.0	-0.4	789	30.0	25.0	-1.6
178	4.9	14.5	9.4	830	17.5	20.0	1.1
211	32.0	29.0	-0.8	865	32.0	24.5	-2.3
251	5.8	14.5	8.0	905	20.5	22.0	0.6
282	28.5	27.0	-0.4	937	32.0	24.5	-2.3
322	7.0	15.0	6.6	978	21.0	21.0	0.0
355	29.0	26.0	-0.9	1008	31.0	24.0	-2.3

Table B-11

Data for $\overline{L}$ = 90 in, $\overline{P}$ = 10 psig, S = 13%, d_o = 0.052 in, $\overline{Q}$ = 23.6 cis, N_{Re} = 12100

f Hz	P_sx100 psi-rms	P_rx100 psi-rms	Gain db	f Hz	P_sx100 psi-rms	P_rx100 psi-rms	Gain db
1	126	122	-0.3	394	8.8	15.5	4.9
2	87.2	84.5	-0.3	427	26.5	24.5	-0.7
4	46.5	45.2	-0.3	467	10.5	16.5	3.9
8	27.5	28.5	0.3	500	27.0	24.0	-1.0
15	16.0	18.0	1.0	538	12.0	17.0	3.0
20	11.5	15.0	2.3	570	27.0	24.0	-1.0
25	8.8	13.0	3.4	612	13.0	17.0	2.3
30	7.6	13.0	4.7	643	26.5	23.5	-1.0
37	6.3	12.5	5.9	684	14.5	18.0	1.9
74	29.0	26.5	-0.8	717	27.0	23.0	-1.4
109	5.0	13.0	8.3	760	16.0	19.0	1.5
140	34.0	32.0	-0.5	789	26.5	23.0	-1.2
179	5.2	14.5	8.9	829	17.0	19.0	1.0
211	31.0	29.5	-0.4	864	28.0	23.0	-1.7
251	5.9	14.0	7.5	903	19.5	20.5	0.4
282	27.5	26.5	-0.4	935	29.0	23.5	-1.8
323	7.2	15.0	6.4	977	20.0	20.5	0.3
353	27.5	25.5	-0.6	1009	28.5	23.0	-1.8

Table B-12

Data for $\overline{L}$ = 90 in, $\overline{P}$ = 10 psig, S = 109%, d_o = 0.052 in, $\overline{Q}$ = 23.6 cis, N_{Re} = 12100

f Hz	P_sx100 psi-rms	P_rx100 psi-rms	Gain db	f Hz	P_sx100 psi-rms	P_rx100 psi-rms	Gain db
1	109	108	-0.1	395	8.1	14.0	4.8
2	78.6	77.5	-0.0	426	24.5	23.0	-0.5
4	48.1	48.1	0.0	468	9.4	15.0	4.1
8	25.9	26.7	0.3	500	25.0	22.5	-0.9
15	15.0	17.0	1.1	541	11.0	16.0	3.2
20	11.0	14.0	2.1	573	25.0	21.5	-1.3
25	8.5	12.5	3.3	616	12.0	16.5	2.8
30	6.8	12.0	4.9	645	24.5	21.0	-1.3
39	5.8	12.0	6.3	688	13.0	17.0	2.3
71	26.5	24.5	-0.7	716	25.0	21.0	-1.5
109	4.6	12.0	8.3	760	14.5	17.0	1.4
142	32.0	30.0	-0.5	792	24.5	21.0	-1.3
180	4.8	13.0	8.7	831	15.5	17.5	1.1
212	28.5	27.0	-0.4	864	26.0	21.5	-1.6
251	5.4	13.0	7.6	904	18.0	19.0	0.5
281	25.5	25.0	-0.2	936	27.0	22.0	-1.8
321	6.7	13.5	6.1	979	19.0	19.5	0.3
354	25.0	23.0	-0.7	1011	27.0	21.0	-2.2

Table B-13

Data for $\overline{L}$ = 90 in, $\overline{P}$ = 25 psig, S = 0.2%, d_o = 0.013 in

f Hz	P_sx100 psi-rms	P_rx100 psi-rms	Gain db	f Hz	P_sx100 psi-rms	P_rx100 psi-rms	Gain db
1	4.8	5.0	0.4	395	0.74	1.85	8.0
2	4.6	4.8	0.3	432	3.3	3.0	-0.8
5	3.1	3.1	0.0	471	0.87	1.85	6.6
10	1.8	2.0	0.9	506	3.2	2.90	-0.9
15	1.15	1.5	2.3	545	1.00	1.90	5.6
20	0.80	1.32	4.3	576	3.4	3.0	-1.1
30	0.37	1.50	12.2	620	1.10	1.90	4.8
35	0.24	1.70	17.0	651	3.3	2.90	-1.1
40	0.41	1.40	10.6	692	1.20	2.05	4.7
70	3.2	3.1	-0.3	721	3.4	3.0	-1.1
108	0.40	1.78	13.0	765	1.35	2.20	4.2
143	3.0	2.83	-0.5	794	3.4	3.2	-0.5
180	0.47	1.67	11.0	829	1.20	2.10	4.8
215	2.73	2.6	-0.5	867	3.6	3.3	-0.8
253	0.56	1.65	9.4	907	1.70	2.40	3.0
289	2.90	2.75	-0.5	939	3.8	3.4	-1.0
327	0.61	1.80	9.4	982	1.90	2.55	2.5
360	3.10	2.85	-0.7	1013	3.9	3.5	-1.0

Table B-14

Data for $\overline{L}$ = 90 in, $\overline{P}$ = 40 psig, S = 0.2%, d_o = 0.013 in

f Hz	P_sx100 psi-rms	P_rx100 psi-rms	Gain db	f Hz	P_sx100 psi-rms	P_rx100 psi-rms	Gain db
1	8.05	8.19	0.2	398	1.10	3.1	8.9
2	7.33	7.57	0.2	432	5.7	5.4	-0.4
4	5.90	6.18	0.4	470	1.30	3.1	7.6
8	3.96	4.34	0.8	506	5.6	5.2	-0.6
10	3.50	3.96	1.2	545	1.50	3.3	6.8
15	1.90	2.45	2.2	574	5.8	5.5	-0.4
20	1.20	2.00	4.5	618	1.55	3.3	6.4
30	0.57	2.40	12.3	648	5.7	5.5	-0.4
34	0.275	2.60	19.5	690	1.70	3.4	6.2
68	5.40	5.4	0.0	718	5.8	5.6	-0.3
106	0.54	2.80	14.3	764	1.90	3.6	5.6
140	5.2	5.0	-0.4	792	5.8	5.7	-0.2
180	0.67	2.70	12.1	832	1.75	3.6	6.4
214	4.8	4.6	-0.4	865	6.2	6.0	-0.3
253	0.79	2.75	10.8	910	2.5	4.2	4.5
288	5.2	5.0	-0.4	936	6.4	6.1	-0.4
326	0.90	2.95	10.4	982	2.8	4.5	4.1
361	5.4	5.2	-0.4	1011	6.6	6.2	-0.5

Table B-15

Data for $\overline{L}$ - 180 in, $\overline{P}$ = 10 psig, S = 0.2%, d_o = 0.013 in

f Hz	P_sx100 psi-rms	P_rx100 psi-rms	Gain db	f Hz	P_sx100 psi-rms	P_rx100 psi-rms	Gain db
1	2.36	2.36	0.0	198	0.52	0.66	2.1
2	1.96	2.06	0.4	216	1.05	0.78	-2.6
4	1.22	1.45	1.5	271	0.59	0.62	0.4
8	0.71	1.02	3.2	289	1.00	0.71	-3.0
12	0.41	0.87	6.5	346	0.64	0.59	--.7
20	0.34	0.79	7.3	362	1.05	0.66	-4.0
25	0.75	0.97	2.2	492	0.77	0.55	-3.0
34	1.55	1.50	-0.3	546	1.10	0.62	-5.0
40	1.05	1.10	0.4	603	0.88	0.55	-4.2
48	0.46	0.83	5.1	620	1.15	0.59	-5.8
53	0.34	0.85	8.0	714	0.96	0.52	-5.4
69	1.30	1.20	-0.7	768	1.20	0.56	-6.6
88	0.40	0.74	5.3	827	0.96	0.56	-4.7
106	1.25	1.10	-1.1	843	1.15	0.55	-6.4
124	0.48	0.78	4.2	880	1.30	0.62	-6.4
142	1.20	1.00	-1.6	896	1.17	0.52	-7.1
162	0.51	0.71	2.9	934	1.25	0.54	-7.3
179	1.10	0.85	-2.3	990	1.45	0.57	-8.2

Table B-16

Data for $\overline{L}$ = 180 in, $\overline{P}$ = 10 psig, S = 0.2%, d_o = 0.013
$\overline{Q}$ = 2.2 cis, N_{Re} = 1090

f Hz	P_sx100 psi-rms	P_rx100 psi-rms	Gain db	f Hz	P_sx100 psi-rms	P_rx100 psi-rms	Gain db
1	2.46	2.65	0.7	216	0.98	0.75	-2.4
2	2.00	2.16	0.7	234	0.54	0.62	1.2
4	1.34	1.57	1.4	289	0.96	0.69	-2.9
8	0.76	1.06	2.2	307	0.58	0.60	0.3
11	0.48	0.88	5.8	326	0.98	0.70	-3.0
20	0.28	0.71	8.1	436	1.10	0.66	-4.3
25	0.88	0.88	0.0	455	0.66	0.58	-1.1
33	1.45	1.40	-0.4	527	0.82	0.56	-3.4
40	0.93	1.05	1.1	545	1.15	0.62	-5.4
53	0.33	0.81	7.8	639	0.90	0.54	-4.6
69	1.25	1.15	-0.7	656	1.15	0.58	-6.0
88	0.39	0.74	5.6	712	0.97	0.53	-5.2
105	1.15	1.00	-1.2	729	1.20	0.56	-6.6
124	0.46	0.63	2.7	857	1.05	0.50	-6.4
142	1.10	0.89	-1.8	879	1.30	0.52	-8.0
160	0.48	0.66	2.1	967	1.32	0.56	-7.5
178	1.05	0.82	-2.2	988	1.48	0.58	-8.2
198	0.52	0.65	1.8				

Table B-17

Data for $\overline{L}$ = 180 in, $\overline{P}$ = 10 psig, S = 7%, d_o = 0.052
$\overline{Q}$ = 23.6 cis, N_{Re} = 11800

f Hz	P_sx100 psi-rms	P_rx100 psi-rms	Gain db	f Hz	P_sx100 psi-rms	P_rx100 psi-rms	Gain db
1	65.7	62.8	-0.4	199	6.5	8.8	2.6
2	39.3	37.3	-0.4	215	15.5	12.5	-1.8
4	21.6	21.2	-0.3	234	7.0	8.6	1.8
8	11.8	11.8	0.0	250	15.0	12.0	-1.9
11	9.41	9.43	0.0	271	7.5	8.5	1.1
21	8.4	7.80	-0.6	343	8.4	8.0	-0.4
26	9.6	8.0	-1.6	359	14.8	10.0	-3.4
37	14.0	9.6	-3.4	485	11.0	7.8	-3.0
45	11.2	8.5	-2.4	506	14.5	8.8	-4.3
57	7.2	7.4	0.3	601	12.2	7.9	-3.7
74	14.5	11.0	-2.4	619	15.0	8.3	-5.2
93	6.3	8.1	2.1	746	14.0	7.5	-5.4
110	16.8	14.8	-1.1	765	16.0	7.9	-6.2
127	6.0	8.8	3.3	895	16.0	7.7	-6.4
145	17.0	14.0	-1.7	912	18.0	8.0	-7.1
164	6.0	8.8	1.1	968	17.5	7.7	-7.1
179	16.0	13.5	-1.5	985	18.8	7.9	-7.5

Table B-18

Data for $\overline{L}$ = 240 in, $\overline{P}$ = 25 psig, S = 0.15%, d_o = 0.020
$\overline{Q}$ = 6.01 cis, N_{Re} = 5030

f Hz	P_sx100 psi-rms	P_rx100 psi-rms	Gain db	f Hz	P_sx100 psi-rms	P_rx100 psi-rms	Gain db
20	1.25	1.59	2.0	217	1.50	1.15	-2.3
25	2.20	2.10	-0.4	230	0.82	0.91	0.9
39	0.42	1.20	9.1	243	1.45	1.10	-2.4
52	2.00	1.85	-0.7	285	0.87	0.87	0.0
66	0.54	1.15	6.6	326	1.40	0.93	-3.6
80	1.95	1.75	-0.9	339	0.89	0.79	-1.1
93	0.59	1.05	5.0	422	1.05	0.73	-3.1
107	1.70	1.45	-1.4	435	1.40	0.79	-5.0
120	0.69	1.10	3.2	505	1.05	0.65	-4.2
133	1.70	1.42	-1.6	547	1.30	0.67	-5.7
148	0.76	1.08	3.0	614	1.10	0.61	-5.2
162	1.65	1.30	-2.1	628	1.30	0.64	-6.2
176	0.78	0.98	2.0	696	1.10	0.56	-5.8
189	1.55	1.25	-1.8	807	1.15	0.54	-6.6
203	0.81	0.97	1.6	917	1.38	0.55	-8.0

Table B-19

Data for $\overline{L}$ = 15 in, d = 0.073 in, $\overline{P}$ = 10 psig, S = 0.2%, d_o = 0.020 in

f Hz	P_sx100 psi-rms	P_rx100 psi-rms	Gain db	f Hz	P_sx100 psi-rms	P_rx100 psi-rms	Gain db
1	2.20	2.20	0.0	250	1.45	2.35	4.2
4	2.30	2.31	0.0	300	1.95	2.20	1.1
8	2.30	2.30	0.0	332	2.10	2.10	0.0
10	2.25	2.25	0.0	360	2.00	1.90	-0.4
15	2.15	2.15	0.0	410	1.90	1.90	0.0
30	2.10	2.15	0.2	470	1.35	1.85	2.7
50	2.05	2.30	1.0	550	0.68	2.10	9.8
80	1.60	2.10	2.3	687	1.75	1.75	0.0
120	1.40	2.80	6.0	740	1.60	1.40	-1.1
160	0.71	3.30	13.3	790	1.45	1.35	-0.6
179	0.48	2.90	15.6	927	0.96	2.00	6.4
210	0.90	2.70	9.5				

Table B-20

Data for $\overline{L}$ = 15 in, d = 0.073 in, $\overline{P}$ = 10 psig, S = 0.3%, d_o = 0.020 in, $\overline{Q}$ = 3.7 cis, N_{Re} = 4450

f Hz	P_sx100 psi-rms	P_rx100 psi-rms	Gain db	f Hz	P_sx100 psi-rms	P_rx100 psi-rms	Gain db
1	3.40	3.40	0.0	250	1.50	2.35	3.9
4	3.20	3.20	0.0	300	2.05	2.25	0.8
8	2.60	2.60	0.0	336	2.25	2.20	-0.2
10	2.45	2.45	0.0	360	2.15	2.05	-0.4
15	2.35	2.35	0.0	410	2.00	1.95	-0.2
30	2.05	2.10	0.2	470	1.50	1.85	1.8
50	2.10	2.20	0.4	550	0.83	2.00	7.6
80	1.90	2.35	1.9	683	1.75	1.80	0.3
120	1.50	2.70	5.1	740	1.65	1.45	-1.1
160	0.85	3.10	11.2	790	1.50	1.35	-0.9
180	0.66	2.85	12.7	829	1.10	1.90	4.8
210	1.00	2.65	8.5				

Table B-21

Data for $\overline{L}$ = 30 in, d = 0.073, $\overline{P}$ = 10 psig, S = 0.2%, d_o = 0.020 in

f Hz	P_sx100 psi-rms	P_rx100 psi-rms	Gain db	f Hz	P_sx100 psi-rms	P_rx100 psi-rms	Gain db
1	1.60	1.60	0.0	210	1.70	1.60	-0.5
4	1.60	1.60	0.0	220	1.70	1.70	0.0
10	1.55	1.55	0.0	240	1.75	1.90	0.7
40	1.30	1.60	1.8	307	0.82	2.10	8.2
70	0.94	2.10	7.0	415	2.15	1.90	-1.1
97	0.50	2.30	13.3	520	0.96	1.85	5.7
86	0.68	2.50	11.3	614	2.20	1.95	-1.0
130	1.05	1.90	5.2	722	1.20	1.80	2.5
170	1.45	1.50	0.3	817	2.15	1.95	-0.8
190	1.55	1.50	-0.3	931	1.65	2.00	1.7

Table B-22

Data for $\overline{L}$ = 15 in, d = 0.073 in, $\overline{P}$ = 10 psig, S = 0.2%, d_o = 0.020 in, $\overline{Q}$ = 2.2 cis, N_{Re} = 2660

f Hz	P_sx100 psi-rms	P_rx100 psi-rms	Gain db	f Hz	P_sx100 psi-rms	P_rx100 psi-rms	Gain db
1	1.60	1.60	0.0	238	1.70	1.80	0.5
4	1.55	1.54	0.0	303	1.00	1.95	5.8
10	1.50	1.50	0.0	412	2.15	1.85	-1.3
40	1.20	1.50	1.9	514	1.15	1.65	3.2
70	0.90	1.95	6.7	612	2.05	1.70	-1.6
97	0.60	2.00	10.4	715	1.35	1.55	1.2
130	1.05	1.70	4.2	823	2.05	1.60	-2.2
170	1.45	1.45	0.0	922	1.75	1.65	-0.5
188	1.50	1.45	-0.3				

Table B-23

Data for $\overline{L}$ = 30 in, $\overline{P}$ = 25 psig, S = 0.3%, d_o = 0.020 in, Vol = 1 cu in

f Hz	P_sx100 psi-rms	P_rx100 psi-rms	Gain db	f Hz	P_sx100 psi-rms	P_rx100 psi-rms	Gain db
1	2.95			316	2.85	0.180	-24.0
5	1.87	1.90	0.0	434	0.18	0.014	-22.2
10	1.70	1.80	0.5	515	2.80	0.145	-25.7
20	1.05	1.30	1.9	645	0.225	0.130	-4.7
40	0.270	0.84	9.9	721	3.20	0.44	-17.2
49	0.075	0.79	20.4	860	0.36	0.30	-1.6
125	2.85	0.90	-10.0	927	3.70	0.88	-13.8
224	0.135	0.175	2.24	1076	0.63	0.60	-0.4

Table B-24

Data for $\overline{L}$ = 30 in, $\overline{P}$ = 25 psig, S = 0.3%, d_o = 0.020 Vol = 2 cu in

f Hz	P_sx100 psi-rms	P_rx100 psi-rms	Gain db	f Hz	P_sx100 psi-rms	P_rx100 psi-rms	Gain db
1	2.95			311	2.80	0.019	-43.4
10	1.25	1.40	1.0	433	0.165	0.065	-9.1
20	0.67	0.97	3.2	515	2.70	0.26	-20.4
37	0.068	0.64	19.4	644	0.215	0.165	-2.3
40	0.130	0.60	13.3	721	2.95	0.52	-15.1
70	0.91	0.43	-6.6	862	0.34	0.33	-0.6
118	2.75	0.47	-15.3	928	3.5	0.90	-11.8
218	0.135	0.065	-6.3	1077	0.59	0.63	0.6

Table B-25

Data for $\overline{L}$ = 30 in, $\overline{P}$ = 25 psig, S = 0.3%, d_o = 0.020 Vol = 5 cu in

f Hz	P_sx100 psi-rms	P_rx100 psi-rms	Gain db	f Hz	P_sx100 psi-rms	P_rx100 psi-rms	Gain db
1	2.95			180	0.56	0.032	-24.9
10	0.275	0.43	3.9	213	0.12	0.039	-9.8
17	0.045	0.295	16.3	311	2.70	0.19	-23.0
20	0.11	0.255	7.3	427	0.17	0.12	-3.0
30	0.39	0.185	-6.5	511	2.50	0.35	-17.1
50	0.87	0.115	-17.6	640	0.205	0.19	-0.6
80	2.05	0.082	-28.0	716	2.70	0.56	-13.6
101	2.70	0.054	-34.0	859	0.29	0.32	0.9
131	1.9	0.004	-53.6	721	3.10	0.93	-10.5
150	1.3	0.014	-39.3	1074	0.50	0.61	1.7

Appendix C

Details of the Apparatus and Procedure

Apparatus Specifications

Detailed specifications of the apparatus outlined in Section III are listed below as follows: name of the instrument, as used in this report, manufacturer, model number (MN) or type number (TN), serial number (SN), range (R), smallest graduation (SG), decade multipliers (DM), and any additional information -- such as the type of operation, accuracy (ACC), linearity (LIN), resolution (RES), etc.

Electric low frequency function generator, Hewlett-Packard, MN 202A, SN 015-07882, R = 1-12^{0}Hz, SG = 0.1, DM = 0.01-100

Electronic counter, Hewlett-Packard, MN 522B, SN 710, R = 0-9999.9 Hz, SG = 0.1, ACC = 0.1 Hz

Pneumatic signal generator, Bendix Research Laboratories, MN TSG-DCC-TS-001

Pneumatic driver, Bendix Research Laboratories, MN PSG 046-B, SN 001

$\overline{P}$ pressure transducer, Consolidated Electrodynamics Corporation, TN 4-313-0001, SN 19148, R = 0-50 psig, LIN - 0.1%, strain gage type with internal bridge

DC null voltmeter, Hewlett-Packard, MN 413A, SN 315-01888, R_1 = 0-3v, R_2 = 0-1v, SG_1 = 0.1, SG_2 = 0.02, DM - 0.001-1000, ACC - 2%, LIN = 0.2%

Vacuum tube voltmeter, Hewlett-Packard, MN 400D, SN 017-43417

P_s, P_r pressure transducer, Kistler Instrument Corporation, MN 701A, SNs 7588, 7591, 946, and 849, R = 0-100 psi, RES = 0.05 psi,

LIN = 0.5%, pizeolectric type

P_s, P_r charge amplifier, Kistler Instrument Corporation, MN 568, SNs 1430, 704, and 1429, LIN = 0.1%

Oscilloscope, Hewlett-Packard, MN H12-175A, SN 10, sweep = 1, 2, and 5 msec/cm, DM = 0.00001-1000; dual trace vertical amplifier, Hewlett-Packard, MN 1755A, vertical sensitivity - 1, 2, and 5 v/cm, DM = 0.001-1, ACC = 3%; scope camera, Hewlett-Packard, MN 196B, SN 422-00793

AC millivoltmeter, North Atlantic, MN 202BR, SN 3469, R_1 = 0-3v, R_2 = 0-1v, SG_1 = 0.1, SG_2 = 0.02, DM = 0.001-100, ACC = 2%

Wave analyzer, Hewlett-Packard, MN 302A, SN 018-01985, R_1 = 0-3v, R_2 = 0-1v, SG_1 = 0.1, SG_2 = 0.02, DM = 0.00001-100, ACC = 5%, R_f = 20 Hz -50 KHz, SG_f = 5Hz, ACC_f = 1% + 5Hz

Flowmeter, Brooks Instrument Company, "Sho-Rate" MM 141-1355, Tube Nos. R-2-15-B and R-6-15-A with stainless steel floats, ACC = 2%

Altimeter, Kollsman, SN 1098, R = 28-31 in. Hg abs, SG = 0.01

Hg in glass thermometer, Wekster, R = -40-120°F, SG = 1°F

Notes on Apparatus and Procedure

As noted by Karem (Ref. 6), many of the problems encountered in a study of this type are not involved with theoretical aspects. Listed below are some of the suggestions from Karem, along with additional items encountered in this study. These notes assume a somewhat greater familiarity with the experimental system than provided solely in this report.

1. Operating manuals are available for all of the apparatus, and usually suggest a short warmup period before taking data. It was found

that at least one hour of warmup is desirable before frequency recalibration is no longer necessary. Also, it was found that electrical baselines of the oscilloscope, charge amplifier combination have a tendency to change between one data session and the next. Recycling the on-off switch usually corrected this difficulty; the equipment was checked and no malfunctions were found.

2. Use coaxial cable only, and use the same type of female and male coaxial connectors. Most of the connectors used in the system were hand fabricated, and different sized cables and connectors were often the cause of lost time spent looking for a poor connection.

3. The Kistler 701A transducers operate best with about a 0.020 in. clearance. The output of the transducers can be affected by their loading, so always use a torque wrench in mounting them; a torque of 20 in.-pounds provides a good seal without overstressing the transducer and fixtures.

It was found that disconnecting the cable from the transducer to the charge amplifier, while the charge amplifier was "on", sometimes resulted in loss of the AC pressure signal on subsequent runs. This condition could be corrected by changing the cable between the charge amplifier and transducer, or waiting for some period of time (for instance, the original lead worked the next day). Therefore, before any leads are changed in the Kistler system, be sure to turn off the associated charge amplifier.

4. Watch carefully for leaks in the test fixture and line connections. It was found that such small leaks do not affect test results, but they do affect signal size.

5. Manufacturer's data supplied with the pneumatic signal generator showed the flatness of the output of the generator to be a function of the electrical signal input. The data supplied with an electrical signal input of 50 volts, showed a rise in output near 800 Hz, and then falling near 1000 Hz; at higher electrical signals the rise was less pronounced. Since very small signals were desired for the tests in this report, the electrical signal input was about 1/5 that used by Bendix. This is thought to be the cause of the response deviation in the vicinity of 800 Hz observed on several of the tests.

6. The 1/8 in. O.D. flowing line tests were characterized by extremely high noise levels (observed on the oscilloscope). One possible source is thought to be the fixture design, since cavity size in the fixtures for this size line were relatively greater than for the 1/4 in. O.D. line.

Vita

Robert Wencel Wilda was born [redacted] the son of [redacted] Graduated from [redacted] in June 1953, he then attended the University of Wisconsin, Madison, Wisconsin, and was awarded the degree of Bachelor of Science, Mechanical Engineering, in February 1958. He was commissioned in the USAF Reserve through the ROTC program. He was employed by the Pratt and Whitney Aircraft Company, Hartford, Connecticut from February 1958 until April 1958, when he entered active duty with the USAF, and was awarded his commission in the Regular USAF. He attended USAF pilot, navigator, electronic countermeasures, and B-52 crew training schools from April 1958 until January 1961. He was then assigned to the 596th Bomb Squadron, SAC, Dow AFB, Maine, as a B-52 electronic countermeasures officer, where he served until his entry into the Air Force Institute of Technology program in May 1965.

Permanent address: [redacted]

This thesis was typed by Mrs. Anna L. Lloyd.

Unclassified
Security Classification

DOCUMENT CONTROL DATA - R & D

(Security classification of title, body of abstract and indexing annotation must be entered when the overall report is classified)

1. ORIGINATING ACTIVITY *(Corporate author)*

AU, AFIT-SE

2a. REPORT SECURITY CLASSIFICATION

Unclassified

2b. GROUP

3. REPORT TITLE

PNEUMATIC LINE DYNAMICS

4. DESCRIPTIVE NOTES *(Type of report and inclusive dates)*

Thesis

5. AUTHOR(S) *(First name, middle initial, last name)*

Robert W. Wilda
Capt. USAF

6. REPORT DATE	7a. TOTAL NO. OF PAGES	7b. NO. OF REFS
May 1967	90	14

8a. CONTRACT OR GRANT NO.	9a. ORIGINATOR'S REPORT NUMBER(S)
b. PROJECT NO.	GA/ME/67-3
c.	9b. OTHER REPORT NO(S) *(Any other numbers that may be assigned this report)*
d.	

10. DISTRIBUTION STATEMENT

Distribution of this document is unlimited.

11. SUPPLEMENTARY NOTES	12. SPONSORING MILITARY ACTIVITY

13. ABSTRACT

The subject of this thesis is the amplitude frequency response (transfer gain curve) of flowing pneumatic lines of the type used in flueric systems. Line lengths up to 20 feet were studied at mean pressures from 10 to 40 psig. The sinusoidal driving signal frequency was varied from 1 to 1000 Hz, and signal size varied from 0.15 to 15 percent of mean line pressure. Test results were compared to proposed mathematical models. The models predicted resonant gain amplitude within 6 db and resonant frequency within 20 percent over the frequency range of 100 to 1000 Hz.

DD FORM 1 NOV 65 1473

Unclassified
Security Classification